Subcontractor Report

PVMaT Improvements in the BP Solarex Photovoltaic Module Manufacturing Technology

**Annual Report
May 5, 1999–June 15, 2000**

J. Wohlgemuth and S. Shea
BP Solarex
Frederick, Maryland

NREL

National Renewable Energy Laboratory

PVMaT Improvements in the BP Solarex Photovoltaic Module Manufacturing Technology

Annual Report
May 5, 1999–June 15, 2000

J. Wohlgemuth and S. Shea
BP Solarex
Frederick, Maryland

NREL

National Renewable Energy Laboratory

NOTICE

This report was prepared as an account of work sponsored by an agency of the United States government. Neither the United States government nor any agency thereof, nor any of their employees, makes any warranty, express or implied, or assumes any legal liability or responsibility for the accuracy, completeness, or usefulness of any information, apparatus, product, or process disclosed, or represents that its use would not infringe privately owned rights. Reference herein to any specific commercial product, process, or service by trade name, trademark, manufacturer, or otherwise does not necessarily constitute or imply its endorsement, recommendation, or favoring by the United States government or any agency thereof. The views and opinions of authors expressed herein do not necessarily state or reflect those of the United States government or any agency thereof.

PREFACE

This Annual Technical Progress Report covers the work performed by BP Solarex for the period May 5, 1999 to June 15, 2000 under DOE/NREL Subcontract # ZAX-8-17647-05 entitled "PVMaT Improvements in the Solarex Photovoltaic Module Manufacturing Technology". This is the second Annual Technical Report for this subcontract. The subcontract is scheduled to run from May 4, 1998 to July 3, 2001.

The following personnel at BP Solarex have contributed to the technical efforts covered in this report.

Fiore Artigliere	Scott Chen
James Cliber	Mark Conway
Tomas Corman	Joseph Creager
George Kelly	Bonnie Kinsey
Timothy Koval	Mohan Narayanan
William Poulin	Steve Roncin
Madhumita Roy	Paul Schneider
Jay Shaner	Stephen Shea
Doug Stark	Mark Susol
Timothy Tomlinson	John Wohlgemuth

BP Solarex has been supported by subcontracts at the Automation and Robotics Research Institute at the University of Texas at Arlington (ARRI), at Specialized Technology Resources, Inc., SiNaF Products, Inc. and the Physics Department at North Carolina State University.

ARRI staff that worked on the subcontract include:

Heather Beardsley	Raul Fernandez
Peter Tanguy	

STR staff that worked on the subcontract include:

James Galica	Norman Sherman
Daniel Wells	

SiNaF Products staff that worked on the subcontract include:

Ronald Gehringer

NCSU worked on the subcontract was performed under the direction of Professor Gerald Lucovsky.

EXECUTIVE SUMMARY

The objective of this three year PVMaT program is to continue the advancement of BP Solarex PV manufacturing technologies in order to design and implement a process which produces polycrystalline silicon PV modules that can be sold profitably for $2.00 per peak watt or less and which increases the production capacity of the Frederick plant to at least 25 megawatts per year. Achieving these major objectives is based on meeting the following specific task goals.

Develop a process to produce silicon feedstock from Na_2SiF_6 that can be sold profitably for less than $15/kilogram in large quantities. Demonstrate the process in a pilot facility.

Optimize and improve control of the casting process to increase the process yield (kilograms of silicon out divided by kilograms of silicon in) by 7% and to improve material quality such that average cell efficiency increases by 4%.

Reduce the center-to-center cut distance on the wire saw to less than 450 μm in production, and develop a wire saw process that reduces the consumable costs by at least $0.05/wafer, that does not require organic cleaners nor result in generation of hazardous waste material.

Develop, demonstrate and implement a cost-effective cell process that produces a minimum average cell efficiency of 15% and improves the cell line electrical yield by 5% when applied to Solarex cast polycrystalline silicon wafers.

Develop and qualify an encapsulation system that meets all technical and reliability requirements and can be laminated and cured in less than 6 minutes.

Improve BP Solarex's product and materials handling (including efforts in at least 3 separate areas) to increase line yield by 3% and reduce handling labor to save $0.05/watt.

Improve process measurement and control in the production line (including efforts in at least 3 separate areas) to improve yield by 3% and reduce rework by 50%.

ACCOMPLISHMENTS

Accomplishments during the second year of the program include:

- Developed processes to produce high purity SiF_4 gas from a number of available commercial sources.
- Designed and implemented a new control system for casting. Added features, alarms and troubleshooting functions, contributed to 4% increase in yield.
- Verified relationship between higher minority carrier lifetime in cast Si and cell efficiency. Now tracking material quality by making measurements of minority carrier lifetime for each production casting.
- Reduced the wire saw pitch to 450 microns with no loss in downstream yield.
- Demonstrated 8% improvement in average cell power on pre-production trial lots using PECVD silicon nitride.
- Developed a new EVA formulation and demonstrated a 6 minute process to achieve adequate cure of PV modules in standard lamination equipment.

- Designed, purchased and installed a new automated assembly line for large area modules. New line reduced rework, increased yield and improved labor productivity by 50%.
- Implemented a factory wide data collection and tracking system. Production volumes and performance parameters are now monitored in real time through the local area network.

TABLE OF CONTENTS

LIST OF FIGURES

LIST OF TABLES

1.0 INTRODUCTION

The goal of BP Solarex's Crystalline PVMaT program is to improve the present Polycrystalline Silicon manufacturing facility to reduce cost, improve efficiency and increase production capacity. Key components of the program are:

- Developing a solar-grade silicon feedstock.
- Optimizing and improving process control in casting.
- Reducing wire diameter and wafer thickness to reduce silicon feedstock requirements.
- Reducing wire saw operating costs.
- Developing a faster cure encapsulant to reduce labor and equipment requirements.
- Increasing cell efficiency and using more robust processes.
- Improving handling and eliminating non-value added handling steps.
- Improving measurement and control throughout the production line.

The results of these efforts will be to reduce PV module production costs so that they can be sold profitably for $2.00 per peak watt or less, to increase the production capacity of the Frederick plant to at least 25 megawatts per year and to improve average cell efficiency to 15%, a secondary effect of which is to reduce the customer's balance of systems (BOS) costs. These goals are to be achieved while improving the already high reliability of today's crystalline silicon modules.

Four subcontractors are supporting BP Solarex in this effort:

1. SiNaF Products, Inc. to work on developing a process and the equipment necessary to produce a solar-grade silicon feedstock.
2. Specialized Technology Resources, Inc. (STR) to develop, qualify and manufacture a faster cure encapsulation system.
3. Automation and Robotics Research Institute of the University of Texas at Arlington to assist BP Solarex in developing equipment for automated handling and improved measurement and control on the production line.
4. North Carolina State University to support BP Solarex in characterizing silicon nitride films and determining how these films can be used to passivate cast polycrystalline silicon.

The baseline for this PVMaT program is the polycrystalline process and production line as it existed at the conclusion of Solarex's previous PVMaT Contract NREL # ZAI-4-11294-01 entitled "Cast Polycrystalline Silicon Photovoltaic Manufacturing Technology Improvements".[1, 2] This baseline is described in more detail in Section 2.0.

The rationale behind this program was to identify specific areas in the baseline process where improvements in handling, process control or the process itself could significantly reduce cost, increase efficiency and/or improve capacity. In addition to these process issues, a materials availability analysis indicated that silicon feedstock must be addressed for the long-term success of crystalline silicon PV.

Most of BP Solarex's (and the crystalline Si PV industry's) silicon feedstock is scrap purchased from the semiconductor industry. Until 1995 most of this material consisted of tops and tails purchased at low cost. In 1995 a shortage of semiconductor grade silicon lead the crystal growers to follow the PV industry lead and reuse their own tops and tails. As the supply of tops and tails

1

dried up, Solarex and the rest of the PV industry were forced to find new sources of silicon feedstock. While this shortage has alleviated due to the down turn in semiconductor sales, the cost has never returned to pre-shortage levels, nor will the available supply of scrap be adequate to meet the needs of an expanding PV industry. Therefore, BP Solarex is working with SiNaF Products, Inc. to develop a solar-grade silicon process to produce the large quantities of silicon feedstock necessary to support growth in the PV industry.

The present casting stations are limited in the amount of data that they can collect and in the number and variety of parameters they can control. Production data shows that average cell efficiency and yields vary considerably from station to station and even from run to run in the same station. Efforts are underway to improve control and to optimize the casting process leading to improvements in both yields (casting and cell line) and material quality, which should translate into higher average cell efficiencies.

The wire saw technology is still evolving and improving. A number of potential changes have been identified that can reduce cost and increase even further the number of wafers/cm of brick that can be cut, thereby reducing the amount of silicon necessary per watt of modules produced.

Work on cell processing is designed to increase the average cell efficiency to 15% (at Standard Test Conditions) while improving process control and reducing the overall module manufacturing cost. Areas of investigation include new process steps (PECVD silicon nitride AR coating and selective emitter diffusion) and modifications to some of the present process steps (doping, edge isolation and screen printing) to develop a more robust process sequence, that is easier to control to achieve higher yields and better efficiency.

The present "Fast Cure" EVA encapsulation system is a significant improvement over the old "Standard Cure" system. However, even with this system, increasing production volume still requires a significant investment in lamination equipment, plant floor space and handling equipment. STR is developing a new encapsulation system, with the goal of reducing the lamination time to less than 6 minutes.

Although most cell and wafer handling functions have been automated or are in the process of being automated, there are still a number of areas in the plant where handling improvements can significantly reduce labor cost and/or improve yield. ARRI assisted BP Solarex in identifying those areas in which improvements in handling can have the greatest impact on reducing cost and increasing capacity.

Improved measurement and control during processing should lead to improved yields and higher average cell efficiency. Three specific areas in the plant have been identified, where additional inline measurements are expected to significantly improve control of the process.

First year efforts in each of these technical areas were discussed in the first annual report[3]. Second year efforts will be discussed in detail in Section 3.0.

2.0 PRESENT PROCESS

BP Solarex's Crystalline Silicon Technology is based on use of cast polycrystalline silicon wafers. The process flow at the end of NREL Contract # ZAI-4-11294-01 is shown in Table 1.[4]

Table 1
Cast Polycrystalline Si Process Sequence

Casting
of
9 Brick Ingots

Wire Saw Wafering

Cell Process
(All Print with Al BSF)

Module Assembly
(XY Positioners)

Lamination
(Fast Cure EVA)

Finishing

The various segments of BP Solarex's module manufacturing process as practiced at the beginning of this PVMaT program are described below.

Casting

BP Solarex has developed and patented a directional solidification casting process specifically designed for photovoltaics [5]. In this process, silicon feedstock is melted in a ceramic crucible and solidified into a large grained semicrystalline silicon ingot. During Solarex's earlier PVMaT program the size of the cast ingot was increased so that each ingot now yields 9 - 11.4 cm by 11.4 cm bricks. This change was implemented in production resulting in a significant reduction in operating costs and in a doubling of the casting capacity at approximately 20% of the cost that would have been required if the same amount of capacity was added by purchasing new casting stations.

Wafering

During the previous PVMaT Program Solarex developed wire saw technology for cutting large area polycrystalline wafers. The major advantages of wire saws are the reduced kerf and increased production volume. During the course of the PVMaT program we demonstrated:
- That each wire saw cuts as many wafers as 22 to 24 ID saws.
- Wire saws can cut wafers on 475 µm centers versus 600 µm centers for the ID saws, resulting in at least 20% more wafers from each cast ingot.
- Wire saws can cut larger wafers (in our case 11.4 cm by 15.2 cm and 15.2 cm by 15.2 cm) while the ID saws are limited by the blade diameter.

Today all of BP Solarex's wafering is performed using wire saws.

Cell Process

The cell process sequence is based on the use of Thick Film Paste (TFP) metallization, where a commercially available screen-printed silver paste is applied as the current carrying grid on the front of the solar cell. This process has been designed to be as cost effective as possible. The high temperature process steps including diffusion, firing of the front and back print pastes and Chemical Vapor Deposition (CVD) of a TiO_2 antireflective (AR) coating are all performed in belt furnaces.

During the previous PVMaT Program, Solarex developed a cost effective aluminum paste back surface field (BSF) process. This process was implemented on the Solarex production line, using a fully automated screen-printing system provided by Baccini. The system is fully operational and has provided a 6.5% increase in average cell efficiency.

Module Assembly

The first part of the module assembly sequence is to solder two solder plated copper tabs onto the front of the solar cells. Solarex procured new automated machines to perform the tabbing operation. Tabbed cells are then laid up into a matrix and the tabs are then soldered to the backs of the solar cells using XY positioners developed in the previous PVMaT program.

Module Lamination

The module construction consists of a low iron, tempered glass superstrate, EVA encapsulant and a Tedlar backsheet. The lamination process, including the cure, is performed in a vacuum lamination system. Then the modules are trimmed and the leads are attached. Finally, every module is flash tested to determine its STC power output.

3.0 PVMAT PROGRAM EFFORTS

The following sections detail the progress made during the second year of the program.

3.1 TASK 8 – Silicon Feedstock Development

In the task 8 effort, BP Solarex worked with subcontractor, SiNaF Products, Inc. to continue development of a process to produce silicon feedstock from commercial grade H_2SiF_6 that can be sold profitably for less than $15/kilogram in large quantities.

There are two distinct production processes that comprise the method under development by SiNaF for the production of solar grade silicon. The two processes are the generation of a high purity gas, and its reduction to form the silicon (Si) and co-produced sodium fluoride (NaF). Most of the work this year focused on the generation of silicon tetrafluoride (SiF_4) gas. Efforts on development of the silicon reduction process were delayed due to funding limitations.

<u>Gas Generation</u>

SiNaF Products, Inc. is considering three raw materials for the production of the intermediate gas. These materials are fluosilicic acid, a by-product of the phosphate fertilizer industry, spent zeolite catalyst, from the petroleum industry, and spent mine and mill tailings, produced as a result of hard rock mining activities. By using production combinations of these three materials, SiNaF Products will be able to rotate production to allow for the lowest price and highest production levels to meet both needs of the solar industry.

Fluosilicic Acid raw material: SiNaF Products has developed a process for producing the silicon tetrafluoride gas from fluosilicic acid by its dehydration with sulfuric acid. During this program year SiNaF Products applied for a patent on this process.

Because of its simplicity, this is the technology of choice for the first development of solar grade silicon. The purity of the gas generated by this technology was demonstrated and reported in the First Annual Report of this contract[3]. Process refinements resulted in the patent filing. Recent work addresses improvements in the safety and the efficiency of gas production. This efficiency improvement resulted in a reduction in the amount of fluosilicic acid required for production of 1,000 MT silicon, from 50 million pounds to 32 million pound.

Current estimate of the fluosilicic acid available from the phosphate fertilizer industry is approximately 100 million pounds per year over capacity. This value does not take into account the current down turn in that industry. With the present process it takes about 32 million pounds of the aqueous acid to produce 1,000 metric tons of silicon. Therefore, the estimated capacity would produce a silicon volume of 3,000 MT. As this production, level is approached transport logistics and price pressure will come to bear.

Spent Catalyst: SiNaF Products has a process patent for the production of silicon tetrafluoride gas from spent zeolite petroleum catalyst[6]. A newly developed process that has streamlined the procedure has superseded this patent. This new technique has lowered the capital operating costs of the process by an order of magnitude. Efficiency has also been demonstrated in the associated metal recovery processes. Plans are to file for a new patent(s) soon.

This work is very timely in another respect. In Feb. 2000 the US Environmental Protection Agency (EPA) issued new guidelines for the disposal of these catalysts and like materials.

The allowable leach ability of the heavy metals has been lowered to a level below that which the current disposal technology can achieve. SiNaF Product's method of utilizing these catalysts will solve this problem for the petroleum refining industry. It is therefore possible that there will be a fee associated with acceptance of this material. If this happens it would mean a negative raw material cost for the production of silicon by SiNaF Products, Inc.

The spent catalyst that is currently being developed is a fluidized cracking catalyst. There is an estimated 300,000 pounds per day being disposed of in our landfills. It takes about 25,000 pound per day of this catalyst to produce 1,000 MT of silicon per year. Therefore, spent catalysts represents a potential source for 12,000 MT per year of solar grade silicon feedstock. In addition to the silicon production, aluminum fluoride and other metal oxide and fluorides are produced as co-produced products. The aluminum fluoride can be sold to the aluminum smelting industry as a primary feedstock. The other metals will be separated and made available for sale into various industries. These plants will either need to have the spent catalyst transported to it or the mineral acid used in its processing. Though seemingly unlimited in its availability, the hazardous nature of the process materials could limit its manufacturing locations and/or provide transportation complications.

Spent Mine and Mill Tailings: A study of the mineralogy of mine tailings has resulted in the identification of this material as potential feedstock for a silicon production plant. The separation of the silica and silicates from the other minerals has resulted in producing a 98% pure material feed for the silicon process. The associated metals have been identified but more work is needed to develop their separation technology.

The "endless supply" of available hard rock mine and mill tailings should provide an unlimited raw material source of silica (SiO_2). One source of this material located in the southwest corner of New Mexico can be delivered for $7.00 per standard ton (equivalent to $10.00 per ton of silica or $20.00 per ton of converted silicon). Most locations are rural and located near railroad routes. Thus taking logistics and hazardous condition out of populated areas. With millions of tons on private and Bureau of Land Management (BLM) lands, this will be the lowest cost raw material for the production of silicon. In addition to the silica and silicates (minerals containing silica), the associated metals and minerals will be concentrated in the process, making them economically viable for further processing. In the long run this raw material could be the primary source of material for the production of solar grade silicon.

Silicon Production

In the SiNaF Products process, the SiF_4 gas is reacted directly with molten sodium to produce silicon with sodium fluoride as a by-product. Materials analysis has shown that the SiF_4 gas produced by SiNaF Products is pure enough to be used directly in the reduction process[3]. The sodium metal is available from DuPont in the purity and quantities required.

Efforts during the second year of the contract involved design of the reduction reactor and its associated safety and handling equipment. While a full pilot plant size (100 Kg batches) has been designed, SiNaF Products, Inc. does not have the capital necessary to build such a system. Demonstration of the silicon reaction process is a key requirement for obtaining the amount of capital necessary to build the larger, pilot system. It was decided that the best route to demonstrate silicon production was to design and build a small research reactor. The design of this research reactor is complete and it is now under construction.

The sodium (Na) melt device will heat a four (4) pound brick of sodium to 110°C to melt it. Dry Argon will be used as pressure to force the molten sodium into the reaction chimney.

Fluorsilicic acid (H_2SiF_6) has been used to generate silicon tetrafluoride (SiF_4) gas. Enough SiF_4 gas to produce a 0.25 kg batch of silicon will be stored in a container. The gas will then travels through a mass flow meter and check valve before entering the reaction chimney.

After preheating the reaction chimney and reaction crucible to above 150°C, the reaction initiation temperature, the liquid sodium and gaseous SiF_4 will react producing silicon (Si), sodium fluoride (NaF), and heat. The cooling fluid of both the reaction chimney and reaction crucible will dissipate the heat. The temperature range for the controlled reaction is between 800°C and 1200°C.

After the reaction chimney and reaction crucible are cooled to room temperature, the reaction chimney will be removed from the reaction crucible. With gas purging, the oven temperature will be increased to the melting point of Si, ≈1425°C to 1450°C. Finally the system will be cooled to room temperature, the lid, the reaction crucible and the contents removed.

The time at temperature in the oven should allow for the consolidation of the Si and NaF in separate phases. With this being the case, the NaF should be chipped away from the silicon ingot. Dwell times and temperatures have to be determined to facilitate this procedure.

After four (4) or five (5) runs, the resultant silicon will be placed back into the reaction crucible, covered with the argon purge lid, heated to a predetermined temperature for a specified time and then cooled to produce a larger ingot with further Si/NaF separation. This procedure should produce ingots in the range of one kilogram for experimentation at BP Solarex.

3.2 Task 9: Casting Optimization and Control

In the task 9 effort BP Solarex is improving control of and optimizing the casting process to increase the process yield (kilograms of silicon out divided by kilograms of silicon in) by 3% and improve the material quality, such that average cell efficiency increases by 1%. This is being achieved by improved definition of the salient casting parameters and implementation of new automated casting control systems.

BP Solarex casting stations have operated with microprocessor controls for a number of years. These units were state of the art when first implemented, but are now obsolete. They are impossible to replace, hard to repair and do not provide sufficient memory for the additional monitoring and control we would like to add to the system. Therefore, the first step in the casting optimization was to replace these controllers with new PC based systems. A new generation, PC based controller was configured and programmed to run exactly the same process as the old controllers. During the first year of the contract, this was installed on a new group of four stations (a quad). This quad was made operational using the new PV based controller.

With the old controllers, the casting process was never fully in control, resulting in a high coefficient of variation (COV) in the downstream processes. An engineering and operations task team was assigned to identify the causes of variation and bring the area under control. The team identified several areas of concern. New work procedures were implemented, along with visual indicators of station status. These were posted on the casting stations and produced better coordination among the operators, engineers and maintenance technicians responsible for the

area. The incidence of failed runs and cracked ingots fell dramatically and remained low resulting in a stabilized coefficient of variation (COV). Overall factory COV showed a more controlled distribution and a slight improvement in the average. Average cell efficiency returned to expected levels. The team then phased out of daily control of the casting, providing revised work instructions and operator training to maintain the progress. However, this effort delayed the introduction of the new controllers onto the remaining stations.

In order to accelerate the transition, a decision was made to begin implementation of the controller upgrades using the existing program, while a software contractor developed specifications, wrote, debugged and implemented the next generation program in a parallel effort.

The first replacement controller included several new features developed under the contract. One station in the quad was equipped with a prototype automatic load/unload unit, a larger bottom heater enclosure prototype, and additional water flow and temperature instrumentation. Two more quads were then switched to the new controllers.

Software was received from the contract programmers to automate station leak testing and gas handling, and permit the saving and loading of recipes to facilitate tailoring of the run parameters for different charge types. Automatic leak detection is now operating on three quads.

An entire new quad has now been added. These units incorporate many of the prototype features developed in the past year, including mass flow controllers and vacuum gauges. The new system performs an auto-leak detect. These stations also incorporate a "second generation" version of the ingot load/unload mechanism, which was prototyped earlier. Unlike the prototype, these lift tables will be controlled by the Opto22 controller rather than a dedicated small PLC. The operator interface consists of a set of illuminated push buttons. The controllers can enable/disable the buttons based on station temperature, and input from the proximity switches and through-beam receivers. Only the enabled buttons will be lit. These stations are shown in Figure 1.

The new stations are equipped with the newly designed large bottom heaters. They produce ingots with a 2 microsecond lifetime cut off, an average of approximately 1.2 cm lower than the older bottom heater design. In addition this design eliminates 1 gasketed joint from the station and employs a newly designed graphite heater element made from a very inexpensive grade of graphite.

The load unload prototype used large pneumatic cylinders to move the lift table out from under the station automatically. The production stations are moved manually with a 'T' bar mounted on the front of the station. The elimination of these cylinders makes it easier to service the station and reduces the cost by approximately $3000 per station. All clamping of the gasketed joint between the bottom heater and the station is done with pneumatic clamps rather than bolts. This eliminates any need for operators crawling under the stations and is therefore much safer.

Major Improvements to the freeze out can were also developed on the prototype. Seven holes in the freeze out can design were eliminated to reduce the possibility of outside air entering the inert atmosphere of the station. The hole in the large steel plate, which is the bottom of the freeze out can, was increased to move the steel further away from the corners of the ingot. This improved the linear growth of the crystals near the side of the ingot and reduced the possibility of creating cracks at the corners of the ingot.

In addition, the insulation package was completely re-designed. The amount of insulation surrounding the ingot was increased for more directional heat flow and reduced power consumption. Average electrical consumption for the heaters was reduced by approximately 1.5 KW average. It is now possible to replace an entire insulation package from below the station without disassembling the station. This will greatly reduce maintenance down time.

Figure 1
New Cast Stations

We have also used the brick lifetime system to establish correlations between average lifetime and final cell performance, (see Figure 2). This allows us to use the brick lifetime measurement itself as the measure of quality for the casting process. In the past, cell performance was used as the measure of quality. This greatly lengthened the feedback loop between casting and the measurement, and introduced noise from the downstream processes. Future casting optimization work will be driven by effects on the brick lifetime.

Figure 2
Efficiency and Current vs Lifetime
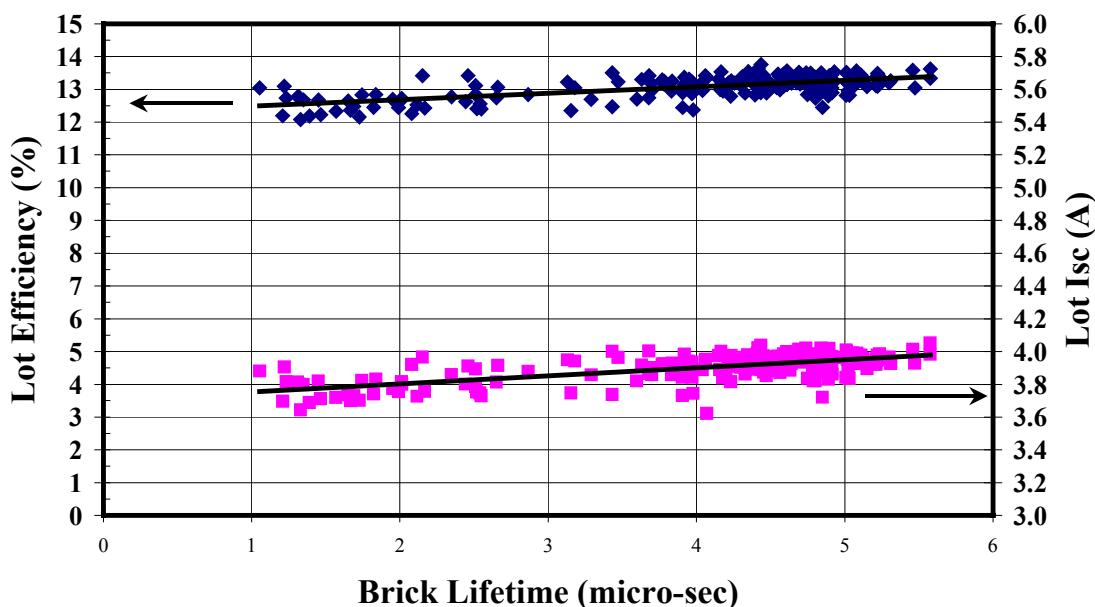
3.3 Task 10: Wire Saw Cost Reduction

In the task 10 effort BP Solarex is working to reduce the center-to-center cut distance on the wire saws in production to less than 450 μm, and is evaluating slurry, oil and silicon carbide recycle approaches.

Wafer Thickness

BP Solarex Operations has completed the transition to the thinner wire without changing the center-to-center spacing.

Reduction of wire guide center-to-center "pitch" was then undertaken in several, incremental steps. In each step, wire guide pitch was reduced a few microns on a single machine and the resulting wafers checked for thickness distribution and downstream yield. Then, the pitch reduction was implemented on all machines, and again the process was monitored for thickness distribution and downstream yield. Equivalent wafer thickness for etched wafers is also measured by weighing all cells processed through the automated screen print equipment in the cell line.

This approach was repeated until the wire guide pitch reached the target 450-micron spacing. We achieved the anticipated increase in saw room yield, but suffered no degradation in downstream process yields during this time. Figures 3 and 4 show the evolution of etched wafer thickness as the wire guide pitch was reduced from 475 microns to 450 microns, followed by the improvement in saw room silicon yield over the past several years. Improvements in saw yield prior to 1999 were dominated by the transition from ID saws to wire saws.

Figure 3

Equivalent Etched Wafer Thickness
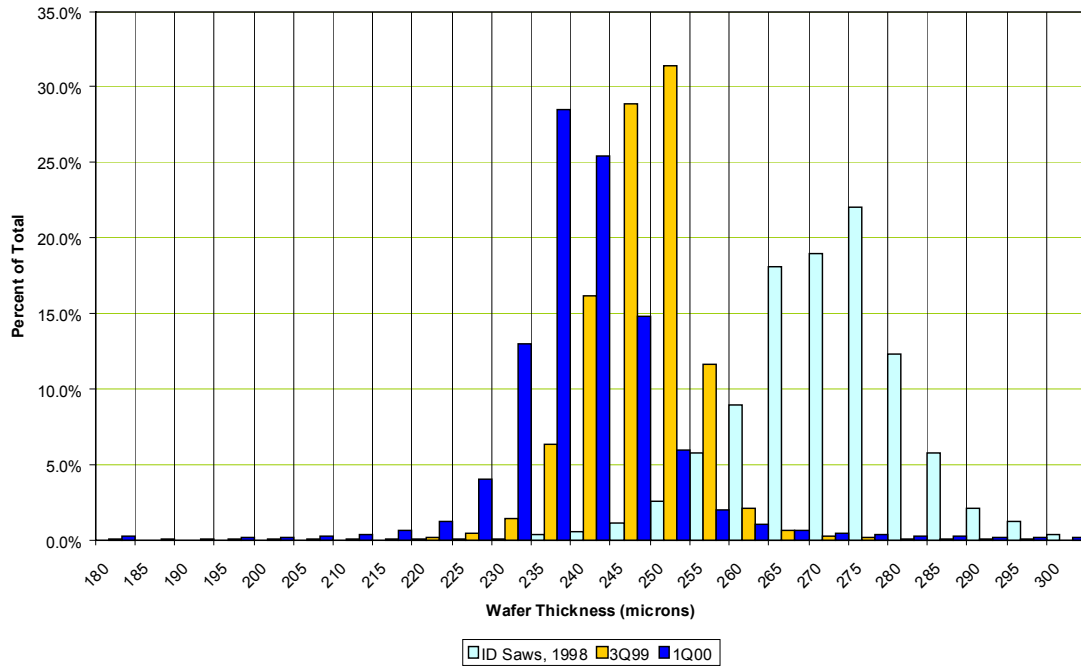
Figure 4

**Sawing Yields (Sq. m Per Sized kg)
Relative to 1993**
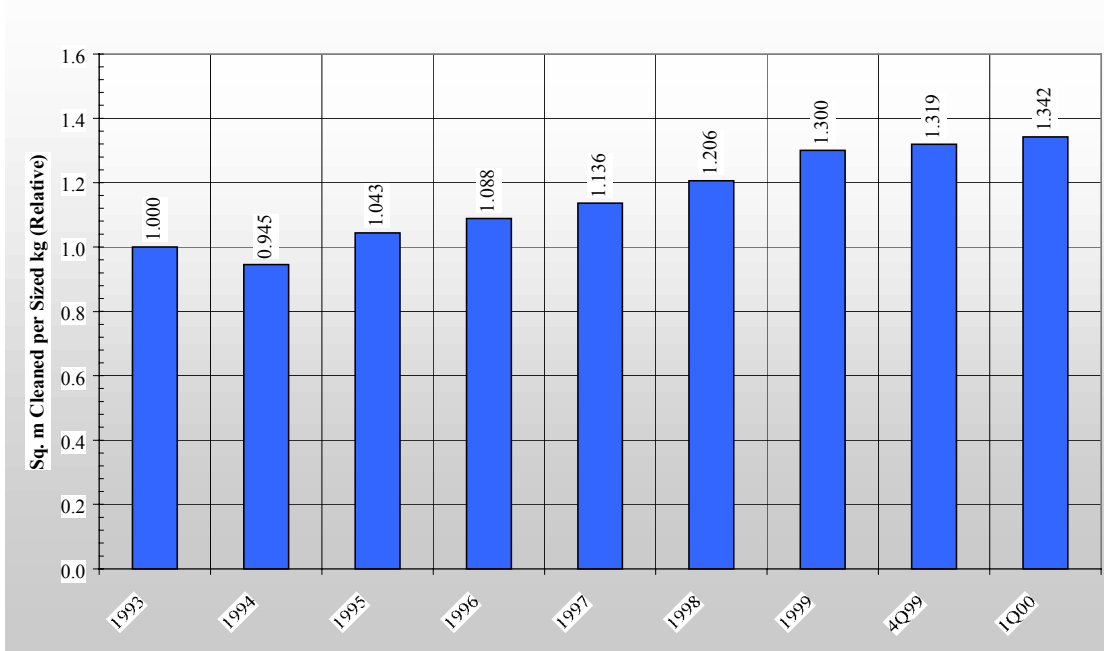
SiC Reclamation

BP Solarex initially leased a reclamation system from GTi. It was a decanter type centrifuge system that extracts the larger particles (SiC) out of used slurry. The solids that are discharged are in a thick sludge or cake form. Fresh oil is added to this cake and is mixed to the desired specific gravity before being used again in the wire saw process.

After achieving acceptable results on the leased system, a production system was installed in 1999. The installed process uses 50% used slurry and 50% reclaimed slurry to make up each manufacturing run, thereby reducing run-to-run variation in the slurry. The GTi system ran very well for over four months, then began running with reduced efficiency because of a worn centrifuge. A new part was installed, but it was determined that the part had to be hard-coated to prevent the premature deterioration of the centrifuge. The part was then replaced with a tungsten carbide tile-coated part, which is expected to have acceptable life.

This system was released to production and is complete.

A second slurry treatment unit, this one from SUI, was also installed on a single machine. This unit was designed to remove silicon fines from used slurry. The manufacturer claimed that the unit could maintain silicon levels within the slurry at 5-8% throughout a cutting run. (Silicon levels after a typical run, are ~10%).

This unit underwent a single day trial. Although the processed slurry was acceptable, the operator interface to the machine was not acceptable. The machine was returned to the vendor for an automation and operator interface upgrade.

The improved version of the machine completed 15 successful runs. Wafer quality remained very stable, and the TTV of the wafers did not drift over time. After fifteen runs the machine suffered a mechanical failure and was again returned to the vendor for redesign.

When the system was returned again it was found to still be unacceptable for a production environment. The machine was returned to the vendor and this approach was dropped.

Glycol-based Slurries

After analyzing the cost savings possible with oil recovery and grit reclaim, this approach no longer appeared to be cost effective and was dropped in favor of oil recovery in 1999. However, environmental and factory cleanliness concerns about oil-based systems have led us to reconsider the introduction of glycol-based systems later in 2000. The existing grit and coolant recovery systems will work with either oil-based or glycol-based coolants.

Oil Recovery

The SiC recovery process described above dramatically reduces the consumption of Silicon Carbide, results in an increased consumption of oil. By feeding the waste stream of the grit recovery system through a decanter centrifuge we have been able to recover clean oil. This product has been tested successfully in several wire saw runs.

The centrifuge system has been integrated with the GTi grit recovery system and is now being run under engineering control. The grit and coolant recovery system is expected to save several hundreds of thousands of dollars a year in materials cost.

Double Table

A prototype brick mounting system was purchased from HCT. The unit allows two bricks to be mounted, side-by-side, on a wire saw, thereby dramatically increasing the throughput of the machine. After overcoming some initial problems with control of the machine during the cut, the first trials resulted in 37% better throughput than the baseline process.

Larger trials continued to show 30%-40% better throughput on the double-table machine, and this equipment has been released to production. One more machine has been converted to the double table system, and two more are scheduled for conversion in the near future.

Wire Re-Use

A fixture was designed to allow re-spooling and subsequent second use of the wire saw wire. The fixture worked very well in engineering trials. However, operator acceptance was poor. At the same time, the double table fixture was coming into production. Wire wear in the double table process is too high to allow reuse of the wire. This approach was then dropped.

Wet Wafer Cassetting

The Wet Wafer Cassetting machine was dropped because the vendor was unable to produce an acceptable design.

Diamond Wire

Laser Tech West is a company located in Colorado Springs, Co. They manufacture a diamond-impregnated wire, which has several possible applications. One is the use of this wire in the wire saw process. This would eliminate the need for slurry and has the potential for faster process times. Two different spools were tested on one wire saw. Neither run was successful. However, the wire appeared to cut well, and the problems were due almost entirely to spool and winding issues. Further tests are planned.

The other possible application is in the Sizing process. The kerf loss in this process is currently close to 4 mm per slice. A process using diamond wire would drop the kerf down to .3 mm, providing very large savings in silicon use and reduced waste streams. A prototype design for a diamond wire-sizing saw is under development.

3.4 Task 11: Cell Process Development

In the task 11 effort BP Solarex is developing, demonstrating and implementing a cost-effective, robust cell process that produces a minimum average cell efficiency of 15% and improves the cell line electrical yield. In the second year, process areas being evaluated and optimized include a new style doper, the selective emitter process, and PECVD silicon nitride antireflective coating (with the assistance of North Carolina State University).

<u>Selective Emitter</u>

One approach to increased cell efficiency is the use of a selective emitter with a deeper junction under the metallization and a shallower junction in the emitter field. In this way the current collection in the emitter can be decoupled from the requirement of the screen-printed metallization to have a high surface concentration of phosphorus. This approach has been evaluated at BP Solarex in the past using masking and etch-back techniques to produce the shallower junction in the emitter field. Efficiency gains in excess of 4% were demonstrated. However, cost analysis indicated that this process is not cost effective[7]. Another approach to achieve a selective emitter is to use a screen printable dopant paste for the deeper diffusion under the metallization area. It was thought that this system might be cost effective, if rapid thermal processing could be used for the light emitter diffusion. For the emitter diffusion, a process was developed that matches the cell efficiency while producing 2.5 times the throughput of diffused cells in the same equipment footprint as the baseline process now in use at Solarex.

We then looked at processes in which we would first print a commercial dopant paste in the pattern to be metallized, diffuse this area heavily, and then add a separate and lighter diffusion to the whole cell. The screen-printed metal can then be applied only in the heavily diffused area. The alignment of the metal to the heavily doped region is critical to the process. We also found that the thickness of the initial dopant print was critical to downstream processing. Thicker layers were not readily removed in the HF step typically used to clean up diffusion oxides before metallization printing.

To address this issue, we tested several new screens for their ability to print the thinnest possible dopant films. At the same time, we tested grid alignment onto a much finer pattern, designed to reduce shading losses and to thereby increase short circuit current. We achieved a 60% reduction in printed dopant paste weight, resulting in a diffusion glass that was barely visible, and easily removed by the standard HF etches. This also eliminated the need for an additional ultrasonic step.

A potential benefit of the very thin film is that it may no longer require a separate HF etch step at all prior to field diffusion. Although the problem of phosglass removal was solved, it created a secondary problem. The previously dark phosglass grid (non- HF etched wafer) was necessary for use as a setup wafer to print the grid metallization precisely over the dopant grid. With the grid now barely visible this is no longer possible. We developed a technique to overcome this problem using the Baccini printer.

Subsequently, trials were run to optimize the sheet resistivity of the field emitter, to obtain maximum current gain without losing too much fill factor. Four different profiles were used to obtain sheet resistivity ranging from 95Ω/sq to 120Ω/sq. A 30Ω/sq dopant paste grid was used for all selective emitter groups.

Best performance showed an increase in current of 1.9% relative to production controls, (see Table 2). However, the FF was down by 3%. (Also note that these cells had poor Voc due to lack of passivating oxide.) This group incorporated a flat 860°C diffusion profile that yielded a 97Ω/sq emitter. Good N-factors and shunt resistances proved that metal grid did not go beyond the finer dopant paste gridline boundaries into the much lighter field diffusion.

Table 2
SELECTIVE EMITTER - RTC TRIAL 5
Field Emitter Varied (100 & 120ohm/sq)

	--N--	EFFIC (%)	ISC (AMPS)	VOC (mV)	FF (%)	RSER (mOHM)	RSH (OHMS)	N FACT.
Unencapsulated results, not corrected for spectral mismatch						*p-values based on a 2-sided t-test w/ df adj. by F-test*		

Control - Standard Production Process - BTU Diffusion (Profile 880°C @22ipm)

	--N--	EFFIC (%)	ISC (AMPS)	VOC (mV)	FF (%)	RSER (mOHM)	RSH (OHMS)	N FACT.
Group 1	--8--	12.50	3.776	586.2	73.4	9.0	26.1	1.28
		(0.23)	(0.051)	(2.5)	(0.6)	(0.4)	(34.9)	(0.03)

30ohm/sq GDP + 97ohm/sq Vapor Doped Field Emitter (Profile 010599_2)

	--N--	EFFIC (%)	ISC (AMPS)	VOC (mV)	FF (%)	RSER (mOHM)	RSH (OHMS)	N FACT.
Group 3	--8--	12.26	3.846	582.3	71.2	12.5	56.3	1.26
		(0.30)	(0.056)	(1.8)	(0.7)	(0.8)	(99.0)	(0.04)
Delta:		-0.23	0.070	-4.0	-2.2	3.5	30.2	-0.02
Delta%:		**-1.9%**	**1.9%**	**-0.7%**	**-3.0%**	**38.8%**	**115.6%**	**-1.4%**
p-value:		.04 *	.01 *	.00 *	.00 *	.00 *	.43	.29

30ohm/sq GDP + 104ohm/sq Vapor Doped Field Emitter (Profile 121198_3)

	--N--	EFFIC (%)	ISC (AMPS)	VOC (mV)	FF (%)	RSER (mOHM)	RSH (OHMS)	N FACT.
Group 5	--8--	11.66	3.808	582.0	68.4	16.9	69.4	1.26
		(0.32)	(0.054)	(2.7)	(1.3)	(2.1)	(64.9)	(0.04)
Delta:		-0.84	0.032	-4.2	-5.0	7.9	43.3	-0.02
Delta%:		**-6.7%**	**0.9%**	**-0.7%**	**-6.8%**	**87.7%**	**165.7%**	**-1.4%**
p-value:		.00 *	.17	.00 *	.00 *	.00 *	.11	.16

30ohm/sq GDP + 115ohm/sq Vapor Doped Field Emitter (Profile 012299_1)

	--N--	EFFIC (%)	ISC (AMPS)	VOC (mV)	FF (%)	RSER (mOHM)	RSH (OHMS)	N FACT.
Group 4	--8--	11.91	3.829	580.1	69.7	14.0	30.7	1.29
		(0.23)	(0.057)	(2.2)	(0.6)	(1.1)	(25.6)	(0.04)
Delta:		-0.59	0.053	-6.1	-3.7	5.1	4.6	0.01
Delta%:		**-4.7%**	**1.4%**	**-1.0%**	**-5.0%**	**56.3%**	**17.4%**	**0.7%**
p-value:		.00 *	.03 *	.00 *	.00 *	.00 *	.75	.50

30ohm/sq GDP + 119ohm/sq Vapor Doped Field Emitter (Profile 012299_2)

	--N--	EFFIC (%)	ISC (AMPS)	VOC (mV)	FF (%)	RSER (mOHM)	RSH (OHMS)	N FACT.
Group 6	--8--	12.03	3.845	582.2	69.8	14.7	37.7	1.25
		(0.26)	(0.054)	(1.8)	(1.1)	(1.4)	(22.2)	(0.04)
Delta:		-0.47	0.070	-4.0	-3.6	5.7	11.6	-0.03
Delta%:		**-3.8%**	**1.8%**	**-0.7%**	**-4.8%**	**63.5%**	**44.4%**	**-2.6%**
p-value:		.00 *	.01 *	.00 *	.00 *	.00 *	.40	.02 *

NO PASSIVATING OXIDE ON SELECTIVE EMITTER GROUPS
CELLS PROCESSED WITH FULL-FIELD BSF BACKS
47 LINE SCREENS - (GDP 1.5Fx1.1B)
30ohm/sq PROFILE (081898_2)

In an effort to improve the fill factor, three new, hotter and faster field diffusion profiles were developed. Sheet resistivities were kept near 100Ω/sq., the optimal result from previous trials.

Junction Characteristics - Spreading Resistance Analysis was performed on 9 polished Fz wafers to compare diffusion profiles for both grid and field emitters. The best grid profile with highest

surface concentration was 012599_1, which yielding a 25Ω/square grid. See Figure 5. The best field profile from this group was 070199_4.

Figure 5
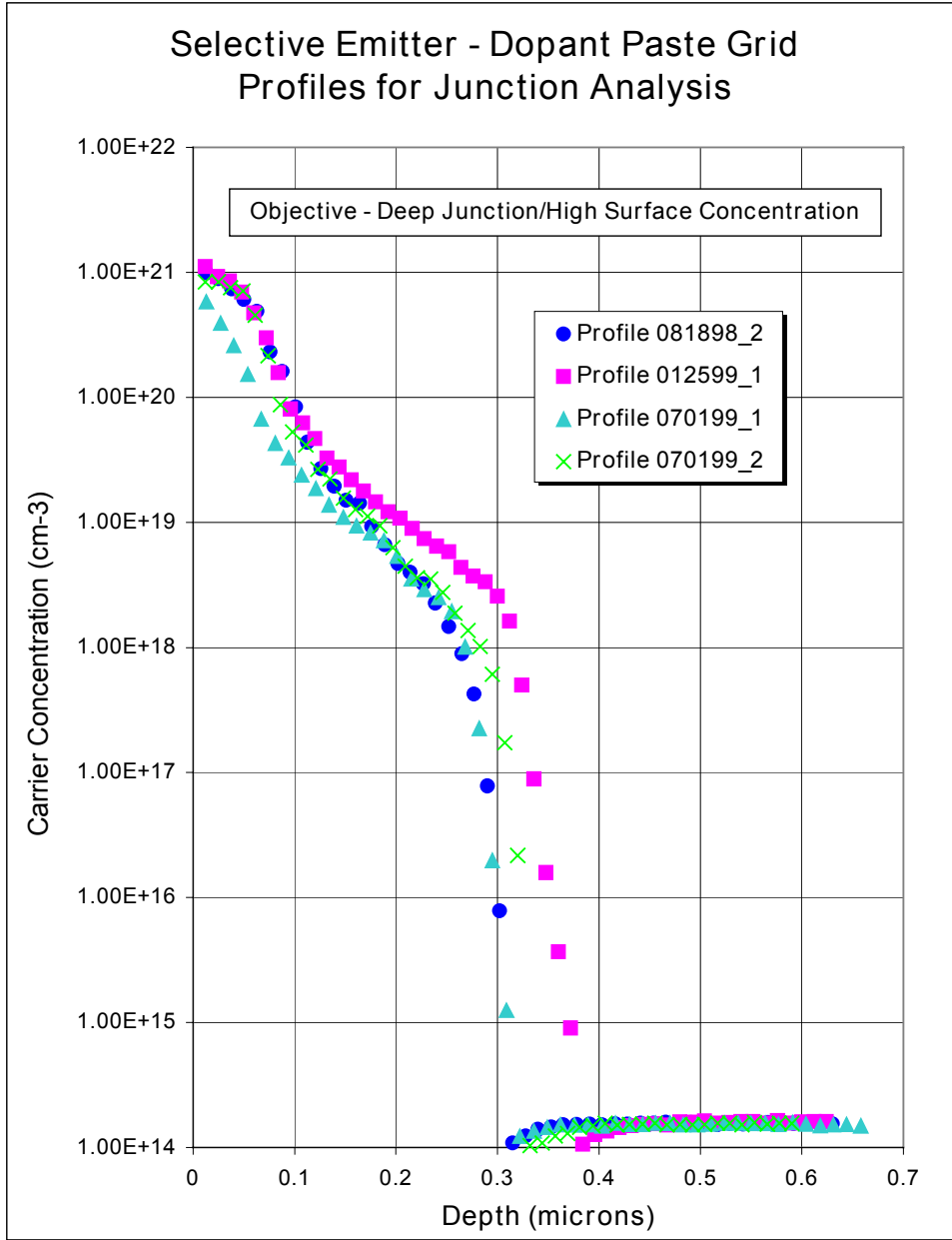
Cell results are shown in Table 3. The best current gain was 1.4% from a 86 ohm/square field diffusion. Despite the lack of a passivated surface, cell efficiency was 1.4% greater than the control group. A passivating oxide could eliminate these losses and yield an efficiency gain of 2-3%. The use of PECVD SiN would provide even further enhancement.

Table 3
RTC - SELECTIVE EMITTER - TRIAL 6
Optimizing Field - Increasing Temperature

	--N--	EFFIC	ISC	VOC	FF	RSER	RSH	N FACT.
		(%)	(AMPS)	(mV)	(%)	(mOHM)	(OHMS)	

Unencapsulated results, not corrected for spectral mismatch   *p-values based on a 2-sided t-test w/ df adj. by F-test*

RTC Control - 44ohm/sq - Vapor Doped - Profile 070698_8								
Profile -->	910	910	910	910	890	880	860	*14ipm*
Group 5	--6--	12.95	3.880	589.8	73.5	9.4	8.8	1.18
		(0.11)	(0.023)	(1.8)	(0.2)	(0.5)	(2.1)	(0.01)

30ohm/sq GDP + 86ohm/sq VD Field - Profile 010599_2								
Profile -->	860	860	860	860	860	860	860	20
Group 1	--6--	12.12	3.936	577.2	69.4	12.0	10.3	1.36
		(0.28)	(0.011)	(4.1)	(1.2)	(0.8)	(2.8)	(0.11)
Delta:		-0.83	0.056	-12.6	-4.2	2.6	1.5	0.18
Delta%:		**-6.4%**	**1.4%**	**-2.1%**	**-5.7%**	**28.0%**	**16.6%**	**15.5%**
p-value:		.00 *	.00 *	.00 *	.00 *	.00 *	.33	.01 *

30ohm/sq GDP + 92ohm/sq VD Field - Profile 070199_3								
Profile -->	900	900	900	900	900	900	900	70
Group 2	--6--	10.85	3.857	557.9	65.5	10.3	8.5	1.83
		(0.72)	(0.025)	(12.6)	(3.1)	(1.3)	(3.0)	(0.39)
Delta:		-2.10	-0.023	-31.8	-8.0	0.9	-0.4	0.65
Delta%:		**-16.2%**	**-0.6%**	**-5.4%**	**-10.9%**	**9.7%**	**-4.0%**	**55.5%**
p-value:		.00 *	.12	.00 *	.00 *	.17	.82	.01 *

30ohm/sq GDP + 91ohm/sq VD Field - Profile 070199_4								
Profile -->	920	920	920	910	890	880	860	75
Group 3	--6--	10.91	3.847	558.8	66.0	10.3	8.3	1.76
		(0.60)	(0.022)	(10.4)	(2.6)	(1.3)	(5.4)	(0.34)
Delta:		-2.03	-0.033	-31.0	-7.6	0.9	-0.5	0.58
Delta%:		**-15.7%**	**-0.9%**	**-5.3%**	**-10.3%**	**9.9%**	**-6.1%**	**49.4%**
p-value:		.00 *	.03 *	.00 *	.00 *	.15	.83	.01 *

30ohm/sq GDP + 92ohm/sq VD Field - Profile 070199_5								
Profile -->	950	925	900	890	880	870	860	70
Group 4	--6--	10.95	3.857	557.6	66.1	10.1	11.4	1.81
		(0.75)	(0.021)	(13.4)	(3.0)	(1.2)	(3.4)	(0.38)
Delta:		-2.00	-0.023	-32.2	-7.4	0.6	2.5	0.63
Delta%:		**-15.5%**	**-0.6%**	**-5.5%**	**-10.1%**	**6.9%**	**28.7%**	**53.5%**
p-value:		.00 *	.10	.00 *	.00 *	.25	.15	.01 *

30ohm/sq Profile (081898_2)

After a review of overall project priorities, work on selective emitter was put on hold. This process, by itself will not be cost effective. Selective emitter designs may be cost effective as part of a high efficiency cell process sequence, but not as a stand-alone addition to our existing process.

<u>PECVD Silicon Nitride</u>

PECVD application of Silicon Nitride (SiN) is a critical component of high efficiency cell processing. The process enhances cell efficiency by providing both an anti-reflection coating and hydrogen passivation of the silicon substrate. Efforts in the previous contract year had focused on first demonstrating the desired efficiency gain, and then on making a set of high-efficiency modules for environmental qualification testing. The cells were diffused at BP Solarex and the SiN deposition and the fire through process were completed at IMEC. Average encapsulated cell efficiency for the SiN modules was 14.6%. These modules passed the standard battery of internal qualification tests.

The next step toward production implementation was to evaluate potential high-throughput equipment. A number of trials were completed with SiN deposited by Shimadzu using their equipment, and completed by BP Solarex or IMEC. Up to 14.5% average efficiency was achieved on small initial trials.

In a subsequent, larger-scale trial, efficiencies over 15% were achieved using wafers diffused at BP Solarex and SiN deposited at Shimadzu, (See Table 4). The metallization was done using a Baccini printer and an RTC furnace.

Table 4

Shimadzu SiN CVD fire through RTC furnace Trial -3

9-Jun-99

	--N--	EFFIC (%)	ISC (AMPS)	VOC (mV)	FF (%)	RSER (mOHM)	RSH (OHMS)	N FACT.
RTC furnace 390/390/833/833/833/833, Belt speed set point 120 IPM								
		15.27	4.352	609.6	74.8	9.1	26.2	1.13
Group 1	--7--	(0.09)	(0.022)	(1.0)	(0.5)	(0.6)	(8.9)	(0.02)
RTC furnace 390/390/836/836/836/836, Belt speed set point 120 IPM								
		15.31	4.370	609.8	74.7	9.2	17.1	1.13
Group 2	--7--	(0.09)	(0.015)	(0.6)	(0.3)	(0.4)	(6.0)	(0.02)
	Delta:	0.04	0.018	0.2	-0.2	0.1	-9.1	0.00
	Delta%:	**0.3%**	**0.4%**	**0.0%**	**-0.2%**	**0.6%**	**-34.7%**	**-0.1%**
	p-value:	.43	.10	.59	.52	.86	.04 *	.90

To evaluate the potential gain of the new process compared to the existing one, an experiment was run to compare the standard cell line process, with BSF and TiO_2 AR coating, to a fire-through process with SiN AR. Both groups went through the BSF process in the production cell line. The SiN fire-through process averaged 7.2 % efficiency improvement over the brick.

18

The spectral response data also shows the improvement with SiN fire through process. A repetition of this experiment produced a 6.8% gain for the SiN fire-through process.

We also investigated the fire-through process on single-crystal substrates. We achieved 16.3% average cell efficiency (measured in air) on 125 mm CZ, SiN fired-through, screen-printed cells. The cell efficiency under encapsulation will be about 16.5%. These efficiencies are comparable to those achieved by the Saturn process (laser-grooved, buried contact process) on similar substrate.

At this point, a detailed cost analysis of the proposed process was prepared, and a technical evaluation was completed for internal management review. Cost and equipment uptime issues with the Shimadzu equipment led us to investigate other potential vendors for the deposition equipment. We decided to focus on the Centrotherm tube furnace as a potentially cost-effective addition to a BP Solarex factory. The tube furnace was found to have higher uptime and lower capital cost per unit output than the in-line equipment used previously.

A 7% improvement in the performance, relative to the baseline process, was demonstrated on wafers with SiN deposited at Centrotherm using the sequential fire through sequence. A system has been purchased. This system should be operational by 4Q 2000 with poly wafers.

New Doper Process

Application of phosphorous dopant at BP Solarex has been done using a patented process in which hot phosphoric acid mist is deposited on the wafer surface just before they enter the diffusion furnace[8]. This process, while very cost effective, is relatively difficult to maintain because the hot acid is hard on the process equipment. A new design was built, using a cool vapor source instead of the traditional heated quartz tube. The reduced temperature relaxes several design constraints on materials used in construction of the doper.

A prototype unit was constructed and used in the process lab to demonstrate performance equivalent to the older method. The lab unit was then used in over a month of extensive, production trials and has been found to have greater reliability than the older units. Production equipment is on order and will be installed later in 2000.

3.5 Task 12: Faster Cure Encapsulant

In the task 12 effort BP Solarex and Specialized Technology Resources, Inc., formerly Springborn Testing and Research (STR), are developing and qualifying an encapsulation system that meets the technical and reliability requirements and can be laminated and cured in less than 6 minutes in the present BP Solarex laminators.

At the request of BP Solarex, a portion of the development effort was directed towards the development of a flame retardant encapsulant system for utilization in standard crystalline silicon PV modules. An improved flammability resistance achieving a minimum UL 1703 Class B flammability rating has been targeted. This is a pioneering effort, as there are no known flame retardant encapsulant systems appropriate to pass the flammability test requirements and appropriate for PV solar cell encapsulation.

Faster Curing EVA-based Encapsulant Development

Throughout this development effort, the industries' desire for a 30-year lifetime encapsulant has been considered an integral part of the requirements. Capitalizing on STR's prior experience in developing UV stabilized, non-discoloring EVA-based encapsulants, every effort was made to select formulation constituents that were felt to have negligible affect on the encapsulant's long-term UV stability[9].

Multiple matrices of experimental formulations were designed to pursue reduction of the encapsulant's cure time. All experimental formulations were prepared using standard laboratory-scale plastics compounding equipment via batch processes. Each experimental encapsulant was laminated using a laboratory vacuum laminator. The construction consisted of the encapsulant sandwiched between two Teflon® impregnated release films, with glass positioned between the platen and sandwiched encapsulant. This construction was felt to closely simulate the heat transfer experienced by the encapsulant during commercial module lamination, for a module constructed with a flexible backsheet. A maximum lamination cycle of six minutes or less, was employed.

Initial screening for viability was accomplished utilizing coupon-sized vacuum laminated samples to determine each formulation's and/or additive's impact on decreasing encapsulant cure time. The degree of cure was measured using standard gel content tests[10] employing hot toluene and/or hot chloroform. Due to the chemical bond formation of some of the final crosslinked compositions, it was necessary to substitute chloroform for toluene to achieve accurate gel content values. For some formulations the toluene had a tendency to swell the encapsulant as opposed to completely dissolving the encapsulant. As a result, the swelled EVA became very sticky and would adhere to the filter media, and result in erroneously low reported gel contents.

Based on the results from gel testing, additional formulations were compounded to improve upon the EVA-based encapsulant's cure rate kinetics. These encapsulant formulations were then characterized for their curing rate kinetics using a Monsanto MDR 2000 Moving Die Rheometer in accordance with ASTM D 6204-97, Standard Test Method for Rubber – Measurement of Unvulcanized Rheological Properties Using Rotorless Shear Rheometers. The rheometer measures the cure characteristics of encapsulants through use of a sealed rotorless moving die system. The encapsulant sample is sealed in a cavity formed by directly heated dies. The lower die oscillates at 1.66 Hz (100 cycles per minute); the reaction torque, measured at the upper die, correlates with the degree of crosslinking as a function of cure time. For each of twelve formulations submitted, including STR's 15295P commercial "fast-cure" control, measurements were carried out at 150°, 155° and 160°C over 12-minute test exposures. Torque versus time is recorded.

The graphic representations of the torque versus time values at 150, 155 and 160°C are depicted in Figures 6, 7 and 8 respectively. As depicted in Figure 6, the control's (15295P) maximum torque was 3.15 in-lb., and required 12 minutes to achieve that level. A maximum torque for the control of 3.21 in-lb. was acquired at 155° in 8.3 minutes and in 6.0 minutes at 160°C. Suggesting that 2% additional cure could have been achieved in some timeframe exceeding 12 minutes at 150°C. The test results further suggests that by increasing the control encapsulant's cure temperature by 10°C, from 150° to 160°C, results in a >50 percent decrease in cure time.
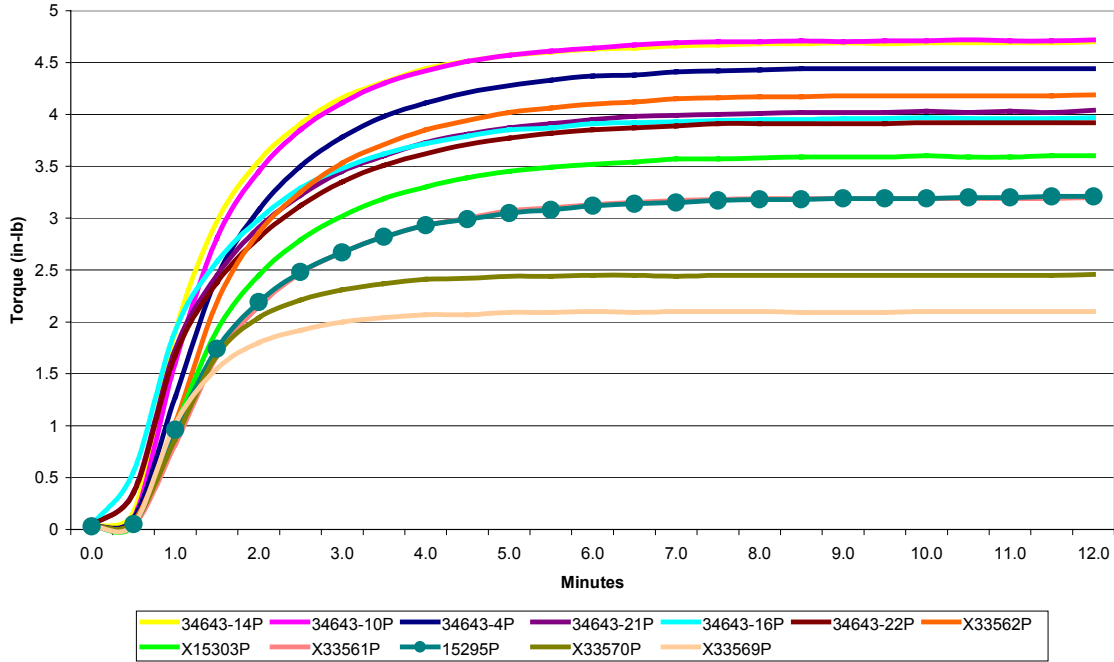
FIGURE 6
Moving Die Rheometry Results @ 150° C
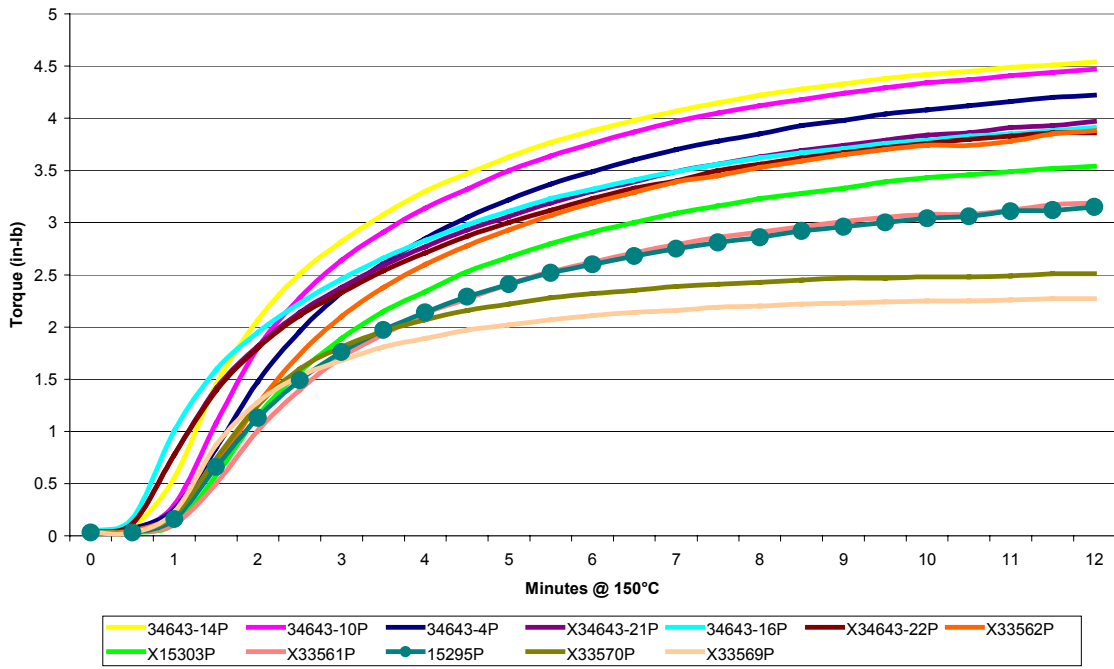
Figure 7
Moving Die Rheometry Results @ 155° C
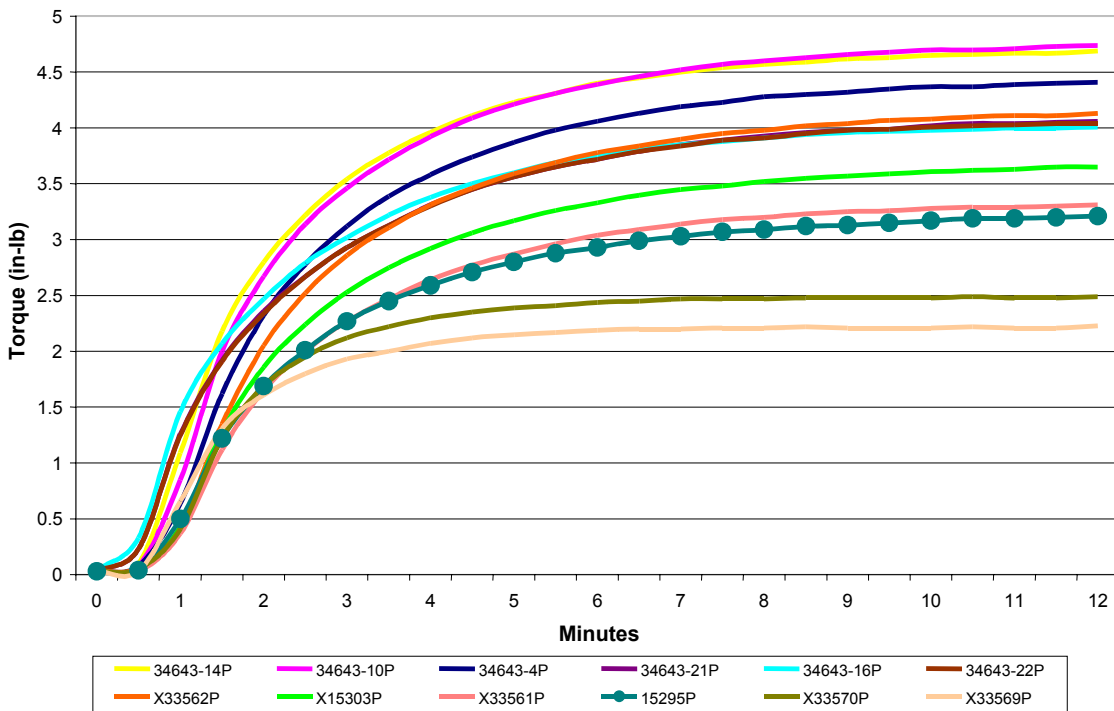
Figure 8
Moving Die Rheometry results @ 160° C

One of the important parameters is peak rate, a function of torque over time. This correlates with the encapsulant's curing rate at the test temperature. At 150°C, the control (15295P) EVA encapsulant has a measured peak rate of 1.1. By increasing the test temperature 5°C, the control's peak rate increased 46%. Raising the test temperature a total of 10°C further to 160° C increased the peak rate by 115% over the 150°C peak rate. The fastest-curing experimental formulation (X34643-14P) tested, demonstrated peak rate advantages of 76%, 79% and 83% versus the control at 150, 155 and 160°C respectively.

In addition to the Moving Die Rheometry results, gel content data resulting from the lamination of test coupons at 140°C, revealed that the experimental EVA-based encapsulants could be cured to the targeted cure levels. Cure levels or gel contents exceeding 70% were acquired in 4 minutes, and 80% in 5 minute lamination cycles at 140°C. The results of those trials are presented in Table 5.

Table 6a, 6b and 6c compare the maximum torque values, as well as the rate and degree of cure for the 11 experimental formulations tested by Moving Die Rheometry and for the control at 150, 155 and 160°C. Each experimental formulation demonstrated varying cure rate advantages, though X33569P and X33570P cured to lower torque values, suggesting that both cure time and cure efficiency are equally important criteria. Experimental formulations X34643-10P and -14P resulted in maximum torque values approximately 45% higher than the control, suggesting a substantial increase in the number of crosslinkage sites, though not necessarily resulting in higher measured gel content. The peak rate, measure of the torque versus time relationship, indicated a 76% gain in cure rate based on X34643-14P at 150°C.

Table 5

Cure Level of Laboratory Laminate Specimens Prepared @ 140°C			
		Gel Test Employing	
Formulation	Cure Time	Toluene	Chloroform
X33561P	6 min.	44%	49%
X33562P	6 min.	63%	70%
X34643-4P	4 min.	70%	78%
X34643-4P	5 min.	80%	84%
X34643-4P	6 min.	85%	87%
X34643-10P	4.5 min.	72%	77%
X34643-10P	5 min.	74%	77%
X34643-10P	6 min.	83%	85%
X34643-14P	5 min.	75%	80%
X34643-14P	6 min.	80%	88%
X34643-16P	5 min.	72%	78%
X34643-16P	6 min.	78%	84%

Table 6a

Moving Die Rheometry Results @ 150°C, 12 Minutes				
	Torque (in-lb)			Peak Rate
Formulation	Min.	Max.	TC 90[1]	(Torque/Time)
15295P Control	0.03	3.15	7:40	1.10
X15303P	0.03	3.54	7:35	1.22
X33561P	0.03	3.19	7:42	1.04
X33562P	0.03	3.88	7:44	1.26
X33569P	0.03	2.27	5:11	1.38
X33570P	0.03	2.51	5:21	1.29
X34643-4P	0.03	4.22	7:37	1.38
X34643-10P	0.03	4.47	7:21	1.75
X34643-14P	0.03	4.54	7:05	1.94
X34643-16P	0.04	3.91	7:15	1.91
X34643-21P	0.03	3.97	7:35	1.56
X34643-22P	0.03	3.86	7:35	1.54

Table 6b

Moving Die Rheometry Results @ 155°C, 12 Minutes			
	Torque (in-lb)		Peak Rate
Formulation	Min.	Max.	TC 90[1]	(Torque/Time)
15295P Control	0.03	3.21	5:36	1.62
X15303P	0.03	3.65	5:37	1.84
X33561P	0.03	3.31	5:36	1.60
X33562P	0.03	4.13	5:40	1.95
X33569P	0.03	2.23	3:30	1.96
X33570P	0.03	2.49	3:36	1.77
X34643-4P	0.03	4.41	5:27	2.13
X34643-10P	0.03	4.74	5:13	2.72
X34643-14P	0.03	4.69	4:58	2.90
X34643-16P	0.04	4.01	5:04	2.78
X34643-21P	0.03	4.06	5:32	2.32
X34643-22P	0.03	4.04	5:24	2.27

Table 6c

Moving Die Rheometry Results @ 160°C, 12 Minutes			
	Torque (in-lb)		Peak Rate
Formulation	Min.	Max.	TC 90[1]	(Torque/Time)
15295P Control	0.03	3.21	3:50	2.36
X15303P	0.03	3.60	3:43	2.72
X33561P	0.03	3.20	3:44	2.32
X33562P	0.03	4.19	3:40	2.89
X33569P	0.03	2.10	2:20	2.53
X33570P	0.03	2.46	2:30	2.43
X34643-4P	0.03	4.44	3:34	3.17
X34643-10P	0.03	4.72	3:22	4.02
X34643-14P	0.03	4.70	3:11	4.32
X34643-16P	0.04	3.97	3:16	3.67
X34643-21P	0.04	4.04	3:36	3.27
X34643-22P	0.04	3.92	3:36	3.19

(1) TC90 is the time it took to achieve a 90% level of maximum torque

Table 7 shows the cure time necessary for each candidate formulation to achieve a similar level of torque or cure versus the control at 150°, 155° and 160°C. The greatest advantage was observed with X34643-14P, accomplishing the control's 12-minute torque level in just 3.6 minutes at 150°C. Other formulations tested offered varying levels of advantages as indicated. Further, the results demonstrate the dramatic affect that processing temperatures has on cure rate.

Table 7

Time To Achieve Full Cure of Control @ Process Temperatures *(3.15 in-lb. Torque)*			
Formulation	150°C	155°C	160°C
15295P Control	12.0 min.	8.3 min.	6.0 min.
X15303P	7.3 min.	4.8 min.	3.3 min.
X33561P	10.8 min.	6.7 min.	5.7 min.
X33562P	5.6 min.	3.5 min.	2.3 min.
X33569P	NA	NA	NA
X33570P	NA	NA	NA
X34643-4P	4.8 min.	4.2 min.	2.0 min.
X34643-10P	4.0 min.	2.5 min.	1.5 min.
X34643-14P	3.6 min.	2.4 min.	1.5 min.
X34643-16P	5.0 min.	3.2 min.	2.2 min.
X34643-21P	5.3 min.	3.5 min.	2.4 min.
X34643-22P	5.6 min.	3.5 min.	2.5 min.

Prototype MSX-60 Module Lamination Trials

Multiple lamination trials were conducted on full-scale Solarex MSX-60 PV modules as qualification for each viable experimental encapsulant.

Initial trials involved fabrication of laminates using a SPI-LAMINATOR™ 350 at platen temperatures of 150°, 155° and 160°C. The laminates employed non-tempered float glass and 11.4 x 11.4 cm polycrystalline silicon wafers in place of actual solar cells. No solder, flux or ribbons were introduced during the initial trials. Craneglas 230 nonwoven glass scrim was incorporated between the substrate side encapsulant and wafers and a Tedlar™ backsheet was employed. The configuration is depicted in Figure 9. Sixteen wafers were used per mock-up, encompassing approximately 40% of the module with cells, and the remaining 60% was cell free.

Figure 9.
Lay-up of the Prototype Laminates
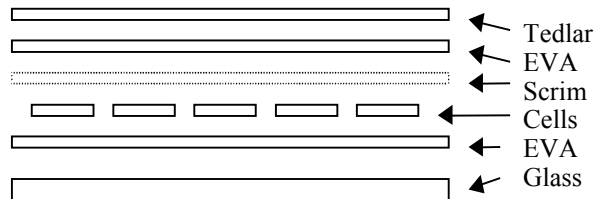
Subsequent lamination trials were conducted utilizing a Spire 240A laminator with an actual solar cell matrix incorporated to fabricate actual MSX-60 PV modules. A broad range of lamination temperatures was studied based on a total laminator process time of 5 and 6 minutes. Cure levels were determined by Gel Content tests using chloroform.

As indicated in Table 8, gel contents as high as 88-91% were measured on samples representative of actual PV modules processed in 6 minutes using PV module components and a standard production laminator. Table 9 indicates that cure levels as high as 80% were achieved using a 5 minute lamination cycles. Modules from this experiment are now undergoing the thermal cycling portion of IEC 1215 as an initial qualification of the level of cure. Through 200 cycles, no evidence of encapsulant failure or movement has been observed.

Table 8
Gel Content for Experimental EVA after 6 minute lamination cycle

Lamination cycle = 6 minutes (105 sec pump, balance press)				
EVA Type	Lamination Temp. (°C)	Temp. Dot (°C)	Avg. Gel Content (%)	Comment
15295P Control	143	132	53	Good
X33561P	143	143	13	Good
X33562P	143	132	59	Good
X33569P	143	132	33	Few small bubbles
X33570P	143	132	71	Good
X33578P	143	132	45	Good
X34643-4P	143	132	91	Good
X34643-10P	143	132	71	Good
X34643-16P	143	132	63	Good
15295P Control	148	143	46	Few small bubbles
X33561P	148	143	43	Blister & bubbles
X33562P	148	143	64	Good
X33569P	148	143	66	Blisters & bubbles
X33570P	148	143	89	Blisters & bubbles
X33578P	148	148	80	Good
X34643-4P	148	143	84	Good
X34643-10P	148	143	88	Good
X34643-16P	148	143	88	Good

Table 9
Gel Content for Experimental EVA in 5 minute lamination cycle

Lamination cycle = 5 minutes (105 sec pump, balance press)				
EVA Type	Lamination Temp. (°C)	Temp. Dot (°C)	Avg. Gel Content (%)	Quality
15295P Control	153	143	74	Bubbles
X33561P	153	143	71	Bubbles
X33562P	153	143	70	Good
X33569P	153	143	73	Bubbles & blisters
X33570P	153	143	71	Bubbles
X34634-10P	153	143	56	Good
X34634-16P	153	143	52	Good
X33578P	157		76	Gel Specimen Only
X34634-4P	157	143	47	Good

UV Stability Characterization of Candidate Faster-Curing EVA Formulations

Samples of X33561P, X33562P and 15295P were laminated between a non-UV screening glass superstrate, i.e. old AFG Solite glass, and window glass. The laminates were prepared in accordance with a standard 15295P lamination cycle. Those samples were aged for 14 weeks in an Atlas Ci-35 Xenon Arc Weather-Ometer for purposes of determining each formulations resistance to discoloration under accelerated fielded conditions. The accelerated aging conditions include a UV exposure at 0.55 watts/m^2 @ 340 nm, at a black panel temperature of 89°C. ASTM D-1925 was utilized to characterize the rate of discoloration by yellowness index. A graphic representation of the UV stability for the 2 experimental formulations versus the control is depicted in Figure 10. Following 14 weeks of accelerated UV aging, both candidate formulations performed substantially better than the 15295P control, with only a minimal increase in yellowness index values, to a level that remains undetectable by eye.

Figure 10

Accelerated Aging Comparison of 15295P, X33061P & X33062P EVA-based Encapsulants by Xenon Arc
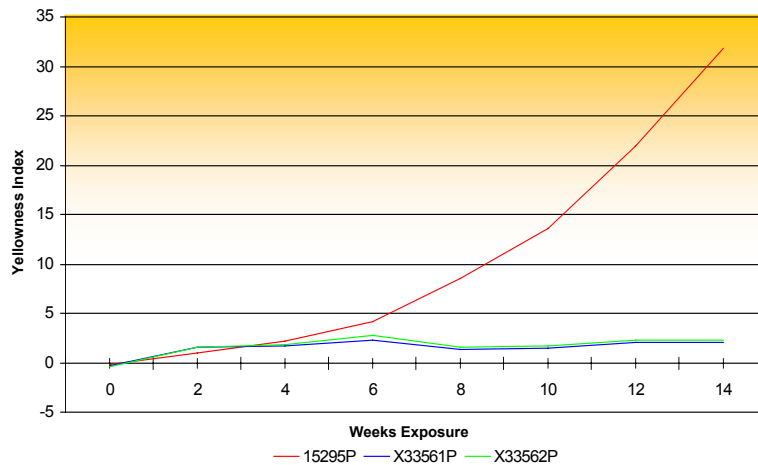
Physical Property Determinations

Following the 6 minute lamination trials, experimental formulation X34643-4P appeared quite promising, yielding a 91% cure level based in a 6 minute lamination cycle. Therefore it was selected for characterization of its key physical properties. The specimens were tested at 80% cure levels. The values of those key physical properties are presented in Table 10. The data suggest that X34646-4P is quite comparable to the control 15295P formulation.

Table 10
Key Physical Properties of X34643-4P Versus 15295P

Property	15295P	X34643-4P
% Light transmission	91	92
Adhesion to glass (lbs.)	43	29
Adhesion to Tedlar (lbs.)	4.4	3.6
Tensile strength	2,100	2,010
Elongation	575	600
Avg. % crosslinking	80	80
Crosslinking time & temp.	10 min. at 150ºC	6 min. at 145ºC
Durometer – shore A	70	69
Tensile modulus (psi)	1,750	1,800

Development of a Flame Retardant EVA-based Encapsulant System for PV Modules

As more PV modules are used in residential rooftop applications, the need for a fire resistant PV module becomes more acute. For practical utilization in a PV module, an acceptable flame retardant encapsulation system would have to maintain a high degree of optical clarity in the encapsulant layer above the solar cells, while the layer behind the solar cells could be opaque. In formulating the flame-retardant system, the additives can not have detrimental effects of the PV modules performance and longevity.

From a chemical property perspective, EVA or ethylene vinyl acetate copolymers are more difficult to flame retard than are polyethylenes. At temperatures exceeding 200°C the EVA encapsulant volatizes acetic acid, which is flammable and contributes dramatically to burning during flammability testing. STR's 15295P "fast-cure" encapsulant can volatilize up to 23% by weight acetic acid at temperatures below 300°C.

The most common flame retardant additives, aromatic halogens, do not react below 400°C and therefore would be ineffective in an EVA-based encapsulant. On the other hand, based on data provided by Albemarle Corp. some aliphatic bromides and chlorides are reactive below 300°C as depicted in Table 11.

Table 11
Flame Retardant Reactivity Temperatures

Albemarle Corp. Product	BCL-462 (°C)	BC-48 (°C)	HBCD (FR1206HT) (°C)	BC-56HS (°C)
1% weight loss	121	137	164	170
5% weight loss	151	167	224	213
50% weight loss	205	224	246	256
Melting point	72	103	186	190

Through laboratory compounding efforts, it was observed that both BCL-462 and BC-48 melt and disperse well in the EVA-based encapsulant. All of the Albemarle flame retardants cited are reactive in the temperature range where acetic acid is being vigorously released from the EVA. Based on a thorough review of the literature and from interviews conducted with a number of commercial flame retardant manufacturers, it became apparent that no commercial flame-retardant additives were considered effective for high vinyl acetate containing EVA copolymers. Most commercial products were specific to the wire and cable industry, and were of little to no value for this PV application.

Common wire and cable practice is to incorporate large concentrations (>50% by weight) of magnesium hydroxide or zinc borate into the plastic. However at a more reasonable loading of 20% by weight for this application, these flame retardants were virtually ineffective.

The information gathering identified three commercial flame retardant systems for possible incorporation into the superstrate EVA encapsulant layer. However, each of those flame retardants systems severely discolored the EVA encapsulant during lamination and were abandoned.

The mechanisms by which flame retardants are suppose to work in high vinyl acetate containing EVA's are:

- Halogenated flame retardant's release the halide as hydrogen bromide or chloride, which intercepts and converts hydroxyl free radicals into water (H_2O), preventing carbon monoxide (CO) from forming carbon dioxide (CO_2).

- The halogen compound or hydrogen halide is inert and envelops the burning zone, excluding oxygen from the air.

- The flame retardant additive is endothermic and releases water or volatilizes, absorbing energy.

- In the case of EVA, a fourth mechanism is use of a basic mineral (pH>8) that neutralizes the acetic acid, forming a less flammable salt.

If a basic mineral were incorporated into the EVA substrate layer, it may partially neutralize the acetic acid that will be released during the flame exposure. It may even act like a chromatographic column to slow passage of acetic acid, diffusing it into the less heated mass and lowering its temperature. Various minerals tested have yielded very different results. Magnesium hydroxide and calcium carbonate have captured the acetic acid, even caused cooling for a few minutes, but eventually burst into flame with vigorous burning. Zinc borate at 20% helped slightly. Zinc oxide helps moderately. Talc and mica do little.

Experimentation that included the incorporation of magnesium hydroxide, calcium carbonate and zeolex into the EVA also catalyzed burning. Other inorganics such as talc and mica offered no advantage. Still others, zinc borate and zinc oxide, demonstrated mild improvement in the EVA's flammability resistance. The most advantageous inorganics evaluated were fiberous wollastonite and very fine silica.

On the basis of internal laboratory test results, the best organic flame-retardants identified were halogen based. Formulations composed of non-halogenated organic flame-retardant systems were not effective in flame-retarding EVA. Formulated at 22% loading they were not effective at preventing combustion, whereas lesser amounts of halogenated flame-retardants, that decompose between 150°C-200°C, were far more effective.

Intrumescent flame-retardants have also been explored and appear to offer the best advantage. Various types of chemical intrumescent systems have been employed as flame retardants by the plastics community for over 50 years. Their effectiveness is directly related to the amount of heat induced during decomposition of the polymeric/organic composition. The thermal decomposition causes the intrumescent system to foam, leading to the formation of a char layer held together by the polymeric composition acting as a binder. Foaming can be as much as 100 fold. The char layer acts as a physical boundary and insulates the composite from the heat source.

There are some concerns regarding the intrumescent systems conductivity and corrosiveness. To evaluate these concerns, samples formulations containing 5%, 10%, 15%, and 20% of intrumescent additives were dispersed into EVA. Surface resistance was measured and ranged from $10^7 - 10^{10}$ ohms (semi-conductive to non-conductive); pH in water was 3.2 initially and 3.1 after one week of immersion. Through addition of alkaline additives, the pH can be returned to neutral or basic.

During the performance of laboratory scale flammability testing using test coupons, it was observed that the Tedlar backsheet may catalyze burning of the PV module. The backsheet's role would be attributed to the high temperature at which the backsheet itself burns. As the flame impinges the front of the module, it causes the EVA to melt and/or burn away clearing the way for the flame to attack the Tedlar. Once the Tedlar ignites, the fire increases in temperature. The increased temperature causes even more rapid deacetylation of the EVA creating fuming acetic acid that is readily flammable.

Similar observations were made when substituting other polymeric films as backsheet. Those included polycarbonate, PET, ULTEM polyetherimide, polysulfone, polyarylate, polyimide, Nylon 4,6, polyphenylene sulfone and polyethylene. Originally it was postulated that these high temperature films might reduce flammability of the module; although the opposite was observed. All appeared to contribute towards vigorous burning by a similar mechanism as observed with the Tedlar.

Experimental flame resistant opaque EVA-based formulations were formulated. UL-94 flammability resistance of plastics, test methods, was utilized to screen the candidates. Laminated EVA specimens withstood direct flame impingement for 15 minutes with no significant burning of the encapsulant.

Alternative lower cost films were substituted for the Tedlar backsheet during flammability testing. Selection was based on films that had sufficiently high melting points to resist deformation during lamination, and also demonstrated substantial adhesive strength the to candidate FR EVA-based formulations. In all cases the candidate EVA encapsulants resisted combustion through 15 minutes of flame impingement.

Flammability tests used standard PV module construction, composed of superstrate glass/ EVA / cells / EVA / substrate film. Fifteen minute resistance to combustion was accomplished utilizing non-FR EVA as the front EVA layer, with FR EVA as the back EVA encapsulant layer. In this

way the optical transparency of the front EVA layer is preserved, thus the FR system presumably will not affect the module's efficiency.

A portion of the flame retardant system is based on the incorporation of intrumescent additive to the EVA encapsulant. Though concerns remain as the additive's pH is 3.1 and its electrical resistivity is 10^9 ohms. The objective is to incorporate this additive into a non-corrosive, insulating encapsulant. Incorporation into an FR EVA formulation has yielded an encapsulant having a pH of 9.3 (after one week's immersion in water), a surface resistivity of 9.3 x 10^{12} ohms/cm and a volume resistivity of 8.6 x 10^{13}. Upon flame impingement, this formulation resisted combustion for 15 minutes, passing our laboratory qualification test.

Based on those results, chemical intrumescent systems have proven most effective at improving the flammability resistance of a PV module. Therefore a number of formulations were developed with the chemical intrumescent system incorporated directly through melt blending into the substrate EVA encapsulant layer prior to manufacture of the encapsulant sheet.

The most promising formulations were utilized to fabricate MSX-60 PV modules. Unfortunately both modules tested failed the flammability resistance test. At this point, further optimization of the flame retardant system is necessary.

3.6 Task 13: Handling

In the task 13 effort BP Solarex is developing improved product and materials handling techniques (including efforts in at least 3 separate areas) to increase line yield by 3% and reduce handling labor to save $0.05/watt. BP Solarex is supported in this task ARRI.

Assembly Automation

The first handling project selected was the development of a fully automated module assembly line. Besides the obvious advantages of automating the process to reduce labor, this line was designed for production of larger modules, up to 240 watts in size, and to minimize the rework and yield losses.

This line is now fully operational. Individual operators handle modules with vacuum lifts, roller tables and flip tables. Modules up to 45 inches (1.14 m) by 75 inches (1.9 m) with weights up to 75 pounds can be produced on this line. Modules are stacked in automatic buffers to avoid damage caused by direct stacking of modules.

The line consists of the following components.

- Glass handling system (See Figure 11)
- Cell tabber (See Figure 12)
- Cell stringing and lay-up equipment (See Figure 13)
- Transport, inspection and lay-up buffer (See Figure 14)
- Automatic load-unload laminator (See Figure 15)
- Transport, rotary table for trimming and light inspection table (See Figure 16)
- Framing system (See Figures 17 and 18)

- Vacuum lift (See Figure 19)
- Inverted solar simulator (See Figure 19)
- Module flip for inspection (See Figure 20)
- Boxing (See Figure 21)

The new line has dramatically reduced the requirements for rework with the number of rejects being reduced by 85%.

Figure 11
Glass Handling Vacuum Pickup

Figure 12
Cell Tabbing Machine

Figure 13
Cell Stringing Machine

Figure 14
Transport, Inspection Table and Lay-up Buffer

Figure 15
Automatic Load-Unload Laminator

Figure 16
Transport Tables, Rotary Table for Trim and Flip Table for Inspection

Figure 17
Framing Magazine and Butyl Pump

Figure 18
Automatic Framing Table

Figure 19
Vacuum Module Lift and Solar Simulator

Figure 20
Flip Table for Final Inspection

Figure 21
Boxing System

Ceramic Handling

As the ceramic pieces get larger and larger, removing them from the molds becomes more difficult. This is particularly an issue for the new single piece crucible. BP Solarex engineering developed a method of removing the crucibles using an inflatable bladder inside of the piece. ARRI utilized this concept to design a fixture for removing crucibles from their molds and placing them onto a drying table.

Various techniques for removing the ceramic crucibles from the molds were studied. Raising and transporting the crucibles using the interior walls appeared to be a feasible approach. The first design approach was to utilize industrial grade inflatable deep-sea lifting bags, customized to meet the requirements necessary for lifting/transporting the ceramic crucibles. The bags are vulcanized in a dry heat autoclave to achieve high strength and durability. Such a unit was procured and tested as reported last year. It was difficult to insert even the smallest unit into the crucible, even while in a deflated state because of the large amount of friction between the neoprene bag material and the inside surface of the crucible. However, once the bag was in place inside the crucible and inflated to approximately 2.5 psi, the crucible could be securely lifted without any difficulties.

It was later found that the simplest and most cost effective method of improving the insertion procedure was to weight the bottom of the airlift bag. This causes the bag to be elongated into a conical shape, which can easily be lowered into the crucible and then inflated.

This handling system was not put into manufacturing, largely because the operators were more comfortable handling the pieces manually. The technique is available for use on larger, later-generation casting stations, where manual handling will no longer be an option.

Slip Dispensing

The focus of this task thus far has been to locate a dispensing system that will meet the need to dispense the slip material for making the grinding balls, lids and spouts. The single most significant dispensing process parameter is fluid viscosity. Viscosity is the proportionality constant relating the speed differential between fluid layers along the direction of flow and the resulting shearing force; it is a measure of resistance to flow. Table 12 illustrates viscosity values for a few common reference fluids:

Table 12
Viscosity of Common Liquids

Reference liquid	Viscosity at 70°C (centipoise)
Water	1.00
Kerosene	3
Hydraulic oil	43
SAE 50 oil	1,100
Molasses	10,800
UV adhesives	60,000
Epoxies	>200,000
Pastes	up to ∞ (no flow)

Equipment is available to handle fluids in the million-centipoise range. The primary effects of increased viscosity, from the perspective of the type of equipment used, is the need to utilize higher pressures and larger orifices to push the fluid, and the potential need for a so-called snuff-back valve or vacuum pull method to avoid *stringing* (and thereby achieve a clean cut-off of the fluid stream). Although UV cured adhesives vary in viscosity depending on the specific formulation, they can be collectively categorized in the medium or moderate viscosity range.

A second key dispensing process parameter is the shot size, which, combined with the net volume of liquid to be dispensed per appropriate time interval (units assembled, hour, shift, day, week), determines whether to use disposable syringe-style barrels or a continuous feed from a reservoir. Equipment exists in both of these configurations to handle volumes from nanoliters to liters. UV cure adhesive dispensing requirements will vary depending upon the application; syringe-style equipment is available to perform high-precision dispensing for small dot applications, while high production rates or high delivery volume patterns (lines and surfaces) must be served by continuous-feed systems.

Fluid viscosity and shot size are the most important of a long list of factors that influence the choice of a dispensing system. Collectively, such parameters may be classified as being related to the fluid characteristics or the manner in which it is to be delivered, as reflected in the list below:

Fluid-related parameters
- Physical characteristics:
    ⇒ Viscosity.
    ⇒ Type (e.g., liquid, gel, suspension, paste...).
    ⇒ Density or specific gravity.
    ⇒ Pot life.
- Is substance tacky or stringy?
- Is viscosity readily affected by heat (e.g., will product flow considerably faster if temperature rises by 10-20 F)?
- Is heating required for proper delivery? What temperature?
- Is agitating required to prevent settling of pigments or suspended solids?
- Is fluid moisture sensitive?
- Must solvent be applied at regular intervals to prevent the substance from "skinning over"?
- Is vacuum degassing required?
- Is fluid corrosive or abrasive?
- Is mixing of two or more components required (e.g., two-part epoxy)?

Delivery-related parameters
- Shot size (cc.)
- Dispense rate (cc/sec.)
- Cycle time (sec.)
- Syringe/reservoir size (cc.)
- Bead application:
    ⇒ Length (mm.)
    ⇒ Diameter (mm.)
    ⇒ Pattern (dot, line, square, circle...)

- Receiving surface geometry (open vs. cavities or bores.)
- Needle gauge or diameter (mm.)
- Reproducibility required (shot-to-shot, stated in +/- % of volume dispensed.)
- How many shots at one time (parallel stations)?
- Is there required post-processing (curing)?

UV cured adhesives are single-part fluids whose curing times are dramatically reduced when exposed to UV light (in the seconds to tens of seconds range.) They usually do not require heating during their application, and are of stable, yet moderate viscosity which can lead to stringing. They are slightly denser than water (≈1.2 specific gravity). Because some formulations also cure in the presence of visible range, the containers and feed lines must be made of opaque materials. In (*non-UV*) light of the fact that curing is required, consideration must be given to integrating the dispensing equipment with a suitable UV source.

There are challenges intrinsic to dispensing. Aside from the parameters previously discussed, there are also application-dependent factors that may influence the specific equipment choice:

- Bubble formation and cavitation; this occurs if the material is being aspired into a chamber with sufficient force to cause it to separate (typical of high-viscosity fluids and pastes.)
- Incompatibility with dispensing equipment material; clogging.
- Exact measurement of liquid dispensed (mass flow) and process verification.
- Abrasive/corrosive materials requiring stainless steel equipment or special valving which uses pneumatic rather than mechanical contact methods.
- Fluid reservoir size and type, refill interval.
- General maintenance: dry air for pneumatic systems, periodic cleaning of wetted components, etc.
- Conflicting parameters: higher pressures and shorter cycle times lead to increased throughput but decrease accuracy and repeatability and require more expensive equipment (high-performance seals.)

Dispensing Equipment Classification

A breakdown of current-day state-of-the-art dispensing equipment by the type of technology used was generated. Table 13 contains a summary list of the categories identified.

Table 13
Dispensing Equipment Classification

Time/Pressure	Positive Displacement
Timed-air pulse syringe (varimeter)	Collapsing tube valve
Dispense (metering) valve	Reciprocating piston
	Rotary valve
	Positive displacement syringe
	Peristaltic pump
	Valve less (progressive cavity) pump

As shown, a logical technology division exists between time/pressure and positive displacement devices. Time/pressure systems rely on the adjustment of fluid pressure and valve open time to allow the passage of fluid, while positive displacement devices rely on the stroke adjustment of

a particular mechanism. The typical tradeoff is initial cost / low maintenance / disposability for the former, versus accuracy / repeatability for the latter.

For the BP Solarex application a Peristaltic Pump was been selected to dispense the slip material.
- Principle: eccentric rotor presses against a pinch tube, creating a vacuum to pull the fluid from the reservoir and pushing it out at the same time.
- Operator unit allows setting the pump speed and cycle time.
- Small shot sizes possible (down to 0.0006 cc.)

- Advantages:
    ⇒ High precision, user-friendly operation.
    ⇒ Self-priming; can retrieve fluid directly from container (no syringe.)
    ⇒ Wetted components easily replaced.
    ⇒ Pump can be operated in reverse to return the fluid in the line back to the reservoir.
- Disadvantages:

Motor unit adds level of complication and lowers reliability.

ARRI tested this dispensing system with BP Solarex slip. From these tests they were able to determine the appropriate dispense rates. The prototype system offers the following features.
- Easy set up and cleaning
- Dispensing rates comparable to current method to dispense balls
- Elimination of the need to carry buckets of slip for lid dispensing process
- Consistent flow rate
- Minimum parts, tube and fittings, come in contact with the slip
- Low cost

Tests of this slip pumping method were satisfactory. ARRI then developed three potential system configurations for improving the slip dispense process. It was agreed to proceed with an enhanced manual method that uses a peristaltic pump and a rack layout that diminishes floor space requirements and is able to shrink current production requirements into a single shift operation. (See Figure 22)

The completed rack holds two rows of six ball molds. Each row has an upper and lower tray for supporting the upper and lower ball mold halves, respectively. Once the molds are loaded into the trays, the trays are clamped to firmly secure the molds. The operator performs the slip dispensing process in the standing position using the peristaltic pump. Once the drying process is completed, the operator raises the tray supporting the upper mold halves with a manually operated winch. For convenient unloading of the balls, the tray containing the lower ball mold halves rotate 180° on a central axis, allowing the balls to drop into a catcher bin. The operator sits on a mobile cart and move along the side of the rack to remove any balls that stick in the lower ball molds.

The completed rack was delivered by ARRI to BP Solarex for testing.

Figure 22
Ball Mold Rack
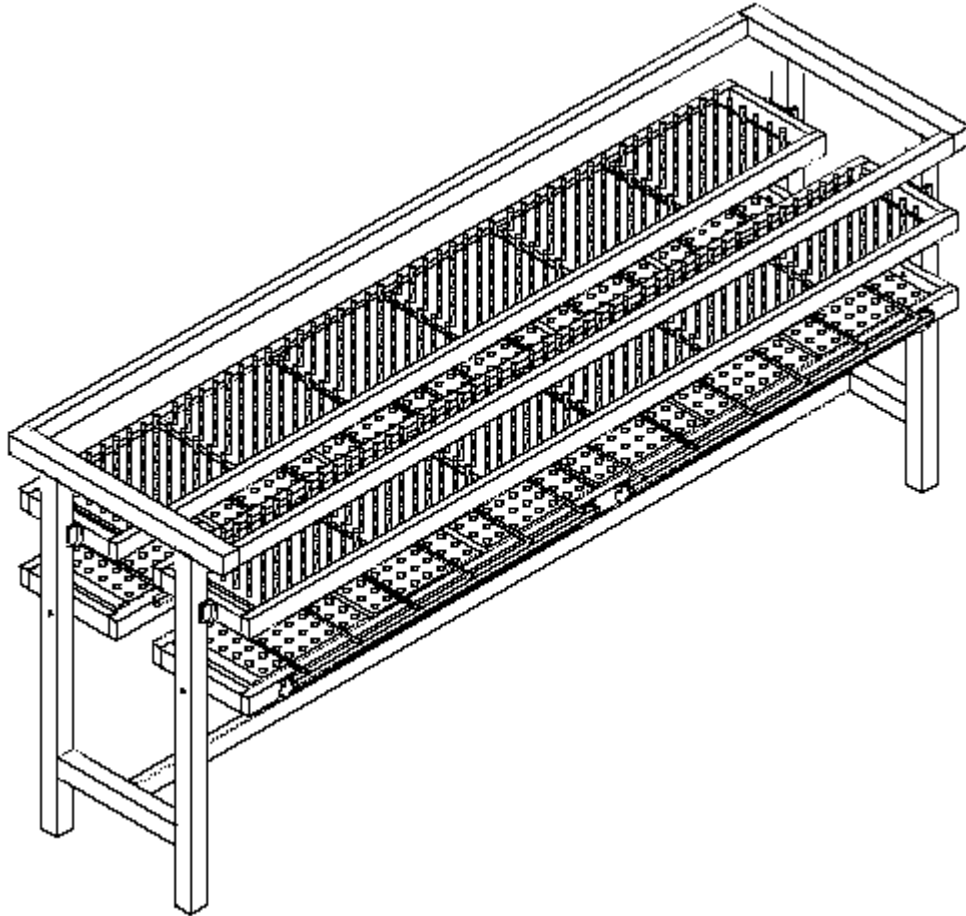
A study of milling ball formation within the mold was also undertaken in order to increase the density of the cast piece and increase the uniformity and working life of the milling balls.

The presence of a central air pocket in the cast milling balls causes them to break up and wear out quicker during mill use. In order to understand the cause of the formation of air cavities within balls, the behavior of the slip during the mold filling process was studied. As the drying process begins, moisture is drawn out of the slip through the walls of the ball mold cavity. In the initial stages, the solidifying slip adheres to the inner walls of the ball mold cavity, forming a thin-walled sphere (Fig. 23(a)). As the drying process progresses, the solidifying slip begins to adhere to the previously solidified slip, and the wall thickness of the sphere increases (Fig. 23(b)). As the slip continues to adhere to itself, a problem begins to develop at the upper fill opening of the ball mold cavity (Fig. 23(c)). The solidifying slip eventually closes off the upper opening of the sphere, trapping a *fixed volume of liquid slip* in the center of the ball (Fig. 23(d)). As the liquid slip looses moisture through the solidified layers and into the mold, an air pocket is caused by the decrease in volume of the trapped slip (Fig. 23(e)).

Figure 23
Stages that occur during the ball drying process, illustrating the formation of a grinding ball and possible development of an air pocket.
(Dots ~ liquid slip, Hatches ~ solidified layers, Blank ~ air pocket)

(a)　　　　　　　　　　(b)　　　　　　　　　　(c)

(d)　　　　　　　　(e)
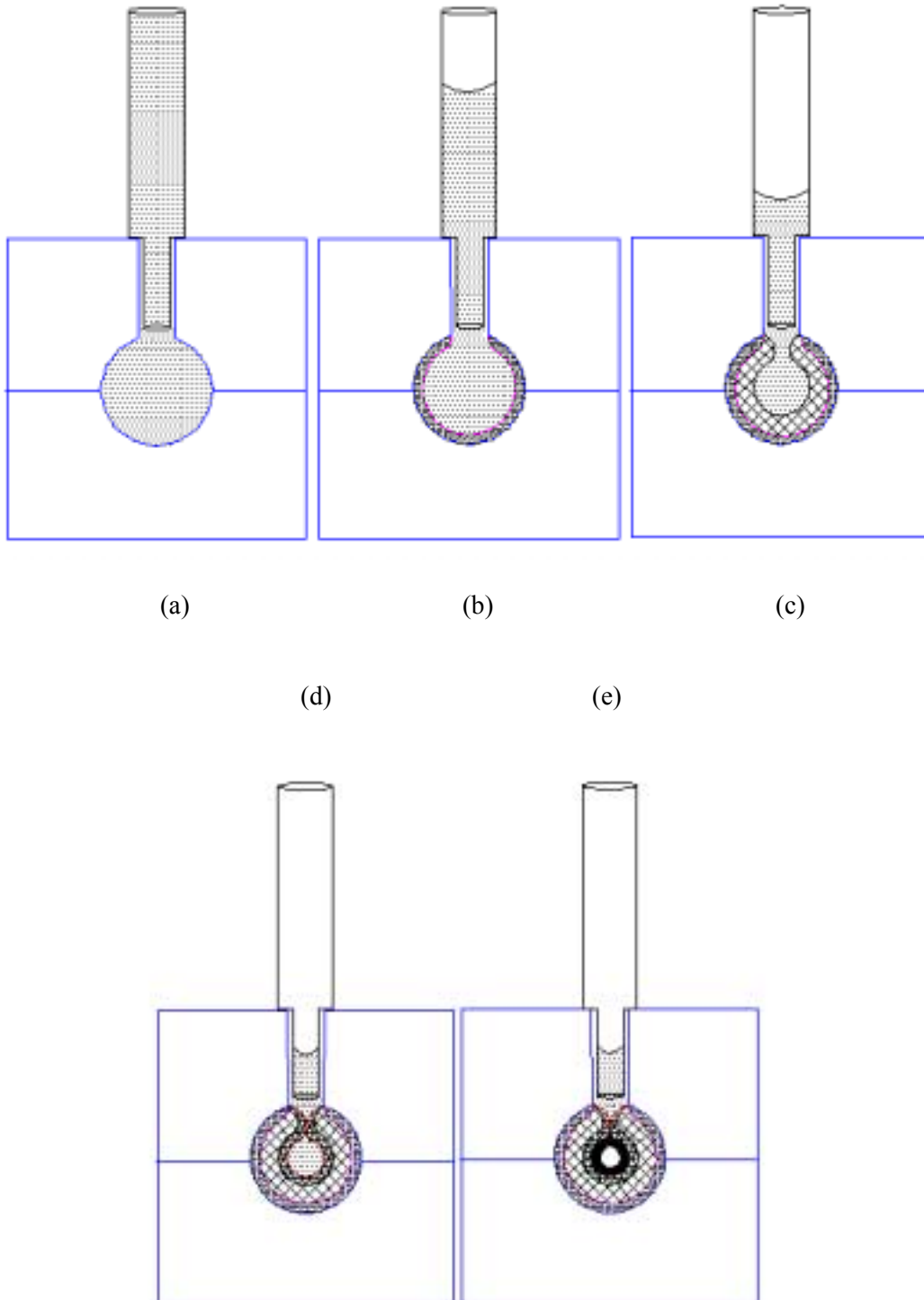
ARRI considered alternative methods for resolving this problem that would allow the solidification pattern of the slip to be controlled, while still maintaining the spherical shape of the grinding balls. These involved either slightly modifying the mold geometry, or making a minor adjustment to the dimensions of the fill tubes. Since modifying the fill tubes was the least disruptive to the slip dispensing process, this approach was tested first.

ARRI modified several fill tubes so the fill neck extends into the ball cavity by 0.5 cm. A slight improvement in the grinding ball formation was observed. The grinding balls formed using the fill tube with the extended neck showed a significant reduction in the volume of trapped air. However, while the large air pocket was reduced to a cluster of star-shaped pores, it was believed that rapid break-up during the mill process would still occur. In an attempt to completely eliminate the presence of any air pockets, the upper half of the ball mold was coated with latex. Thus, drying could occur only through the lower mold half. This would force the solidification process to occur from the bottom upward rather than radially. The resulting grinding balls were completely solid, exhibiting no air pockets or pores.

Handling in Casting

This task has been broken down into two parts. The first part involved a Solarex redesign of the casting station to allow for automatic ingot unloading of the station. This task was begun during the first year, with a prototype unit designed and built by an outside vendor. This unit was installed and tested during year two of the program. Modified versions of the prototype wee then installed on the new quad described in Section 3.2. Photographs of the new handling system are shown in Figures 24 and 25.

Figure 24
New Ingot Loading Cart – Extended
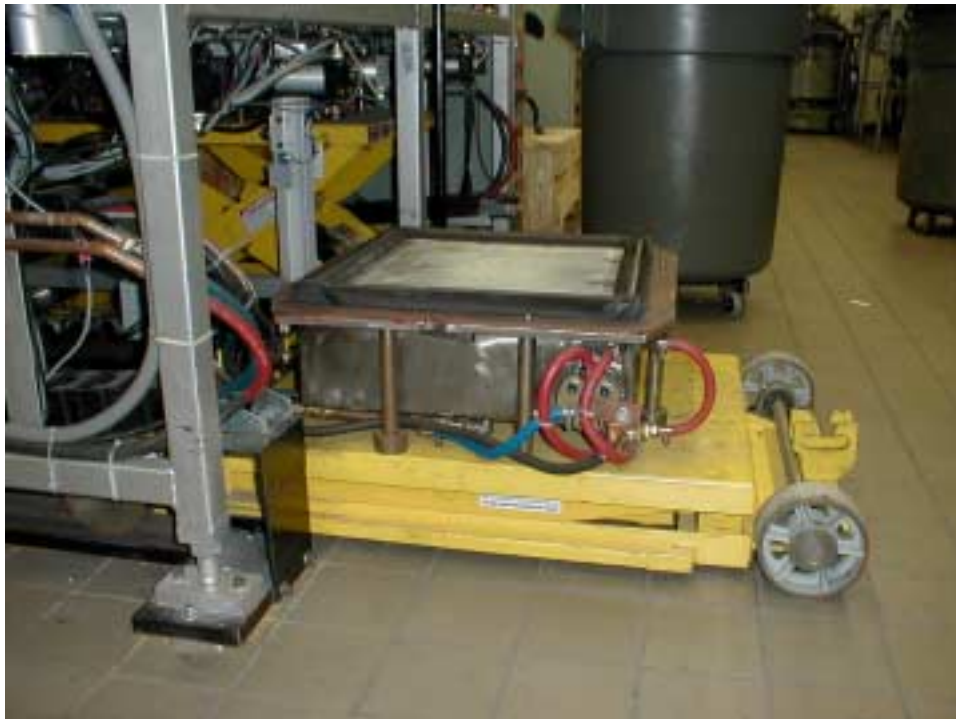
Figure 25
New Ingot Loading Cart – In Place

3.7 Task 14: Measurement and Control

In the task 14 effort BP Solarex is developing process measurement and control procedures for use on the production line (including efforts in at least 3 separate areas) to improve yield by 3% and reduce rework by 50%. In order to improve process measurement and control in the production line and reduce rework BP Solarex, with support from a lower-tier subcontract with ARRI, has implement an improved information system, performed a factory measurement and control survey to determine what areas require improvement and selected 3 measurement and control projects for implementation in the program.

Brick ID System

One approach to improve data collection would be to mark and track each wafer. Our plan was to develop a process whereby the face of every silicon brick is marked before wafering. Hopefully, these marks would be readable on the wafers all the way into the finished product and identify the brick from which each wafer came and its position within the brick. In the first year of the

program, we found a vendor, who was able to scribe very shallow but easily sensed troughs along the brick edge. The bricks were then wafered without yield problems run through the cell line. Cell line yields were acceptable. However, the scalloped edges of the trough were visible in finished laminates and were not thought to be cosmetically acceptable. This work was halted as having a low probability of success.

Doping and Diffusion Measurements / MES

There was consensus of the Solarex engineering staff that diffusion was the most important place to begin improved measurement and control. A prototype measurement and control system for the diffusion area was proposed. ARRI identified the sensors, computer hardware and software necessary for such a unit.

In the first contract year, ARRI assembled a prototype unit with sensor interface modules for thermocouples, frequency counters and generic RS-232 interfacing (such as digital scales, bar code readers, digital voltmeters, etc.). A major issue involved the wafer sensor selection and placement for counting. ARRI identified a potential source that eventually resulted in procurement of a sensor that could identify and therefore count silicon wafers.

A prototype system was partially deployed in Year 2. Hardware was installed on the line, and a preliminary operator interface was set up. At that point the deployment was stopped due to uncertainty about how to interface the system with the rapidly evolving internal computer network, the specifications of which were likely to change because of the information systems requirements of our new parent company.

Instead of tackling this problem at the single node of diffusion, a generic approach was taken. This resulted in the deployment of a plant-wide, prototype manufacturing execution system (MES). The system is in the form of an intranet web site, collecting data from a number of nodes around the Frederick factory.

The site is still under development, but offers a great deal of real-time information. The site is accessible from any computer within the Frederick plant and in a few special cases the site can also be viewed from out side the plant. Because an Internet Browser is the only software needed to view the site, cost is kept down while providing all users with the same data presented in a consistent and easy to use form. Most of these pages are dynamic, automatically updated with the most recent data each time the page is visited.

Pages exist for most of the areas in the process. Information is available for Casting, Sizing, Wafering, Cleaning, and Cell Line, among others. The page for each area typically shows how much product was made at each process, what is the yield for each process and what are the yield losses. Most processes also show the Coefficient of Variation (CoV). Some of the pages allow viewing of specific information that is user selectable. For example, on the cell line page, the user can select a particular period of time, or a particular cell size or a particular line – Baccini or Manual line. Most pages present the information in tabular form, but many also allow the user to display the information in graph form.

Vision Inspection of Solder Tab

Uniformly reliable solder bonds between module interconnect ribbon ("tabbing ribbon"), and the front and rear cell metallization, are critical to the long-term field reliability of PV modules. Present manufacturing practice relies on destructive testing of sample bonds to control the

soldering process. This practice is expensive, and limited sampling runs the risk of missing potentially defective joints. ARRI and BP Solarex this year began to look for a method by which the solder joints might be effectively 100% tested using a non-destructive method.

The first approach was to apply automated vision inspection of the tabs, looking for signatures characteristic of good or of unacceptable joints.

It was determined that a vision system with standard vision tools was capable of measuring the amount of surface area where the solder had re-flowed along the tabbing ribbon (see Figure 26). The length of re-flow, or "met-back" of the solder is an indication that the ribbon received the correct amount of heat during the soldering process. This is true for top and bottom solder joints.

Figure 26
Solder Reflow Inspection Using Vision System
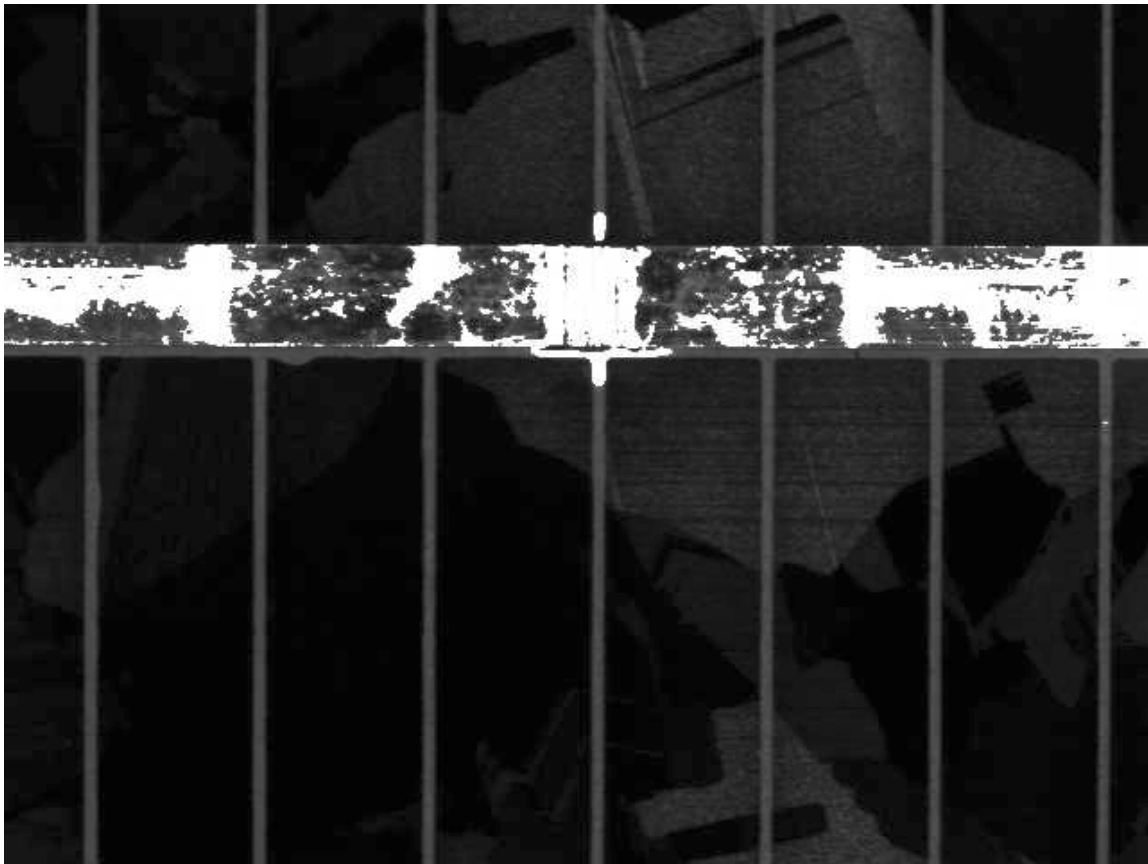
However, additional testing showed many cells solder joint signatures that were not clearly discernible by machine vision, even after trials with several different structured lighting configurations.

The vision approach was subsequently dropped in favor of infrared sensing. ARRI has obtained an infrared camera and will set up a soldering test-fixture in their facility to pursue this concept.

Wafer Fracture Detection

Wafer breakage during processing is a very high cost issue. This is particularly true when wafers fail during one of the print steps, generally resulting in several minutes of downtime while the operator cleans up the scattered parts and the wet paste. This is also a source of potential contamination. It is believed that wafers frequently fail at the print steps, not because they come into the process already cracked and the crack then fails when it is stressed during the process step. ARRI and BP Solarex are investigating methods for detecting and rejecting cracked wafers before they are processed.

Several potential methods and vendors were identified initially.

Eddy Current Testing

Identified a company that claims they are using eddy currents successfully to detect micro cracks in wafers. Eddy current sensing is fast enough for on-line use and less costly than ultrasonic testing.

Samples of good and of damaged solar cells were submitted for eddy current testing. The supplier reported that wafers that have not yet been through the metallization process tend to yield better readings, however they went ahead with the testing. The metallization gave a signal of ~100,000. The silicon produced a response of ~1000 and a flaw response of ~10. Variations in the metallization will tend to swamp any flaw response. A multi-frequency eddy current system may produce better results if testing is to be done on metallized cells, but this method does not appear viable.

Laser-based Ultrasound

This method is based on using a short laser pulse directed at the wafer to cause a sudden rise in temperature of the wafer material. The temperature rise initiates a sudden but minor expansion of the silicon. The acoustic energy released from the expansion can be used to distinguish between elastic or plastic expansion. The strain energy emitted from the cracks will produce acoustic waves having frequencies characteristic of plastic deformation.

The technique is fast enough so it can be implemented on-line, is a non-contact approach and can be described as "low-cost."

Cells were also sent to test the feasibility of using Laser Based Ultrasound (LBU). The vendor demonstrated that laser-based ultrasound inspection is a viable method for detection of micro-cracks in wafers. The inspection technique involves the use of two lasers. The first laser scans the wafer in 5-mm increments along the x and y directions to create localized heating of the wafer, which causes the targeted region to expand, emitting acoustic signals. The acoustic emission is measured by the second laser, which takes the place of contact sensors normally used in acoustic emission sensing.

REFERENCES

[1] J. H. Wohlgemuth, "Cast Polycrystalline Silicon Photovoltaic Module Manufacturing Technology Improvements" Final Subcontract Report, NREL/SR-520-26071 – June, 1999.

[2] J. H. Wohlgemuth, D. Whitehouse, T. Koval, J. Creager, F. Artigliere, T. Tomlinson, J. Cliber, A. Buckman, M. Perry, S. Narayanan, S. Shea, M. Roy, G. Kelly, M. brisson, R. Dominguez, amd M. Conway, "Progress in Solarex's Crystalline Silicon PVMaT Program, *Proceedings of 26th IEEE PV Specialist Conference,* p. 1055, 1997.

[3] J H Wohlgemuth, "PVMaT Improvements in the Solarex Photovoltaic Module Manufacturing Technology" First Annual Subcontract Report, NREL/SR – in press, 2000.

[4] J. H. Wohlgemuth, "Cast polycrystalline Silicon Photovoltaic Cell and Module Manufacturing Technology Improvements", *NCPV Photovoltaic Program Review,* AIP Conference Proceedings 462, p. 747, 1998.

[5] J.H. Wohlgemuth, "Casting Polycrystalline Silicon for Photovoltaics", Proceedings of   International Symposium-Workshop on Silicon Technology Development and Its Role in the Sun-Belt Countries, 14-18, June 1987, Islamabad, p. G-1.

[6] R. Gehringer, "Method for Hydrofluoric Acid Digestion of Silica/Alumina Matrix Material for the Production of Silicon tetrafluoride, Aluminum Fluoride and other Residual Metal Fluorides and Oxides", US Patent 5,242,670, 1993.

[7] S. Narayanan and J. Wohlgemuth, "Cost-benefit analysis of High-efficiency Cast Polycrystalline Silicon Solar Cell Sequences", *Progress in Photovoltaics*, Vol. **2** No **2**, p. 121, 1994.

[8] T. Koval, "Vapor deposition of H_2PO_4 and formation of thin phosphorus layers on silicon substrates", US Patent 4,360,393, 1982.

[9] W. Holley, S. Agro, "Advanced EVA-Based Encapsulants" Final Report, NREL/SR-520-25295, September 1998

[10] PHOTOCAP Solar Cell Encapsulants, Technical Guide

REPORT DOCUMENTATION PAGE

Public reporting burden for this collection of information is estimated to average 1 hour per response, including the time for reviewing instructions, searching existing data sources, gathering and maintaining the data needed, and completing and reviewing the collection of information. Send comments regarding this burden estimate or any other aspect of this collection of information, including suggestions for reducing this burden, to Washington Headquarters Services, Directorate for Information Operations and Reports, 1215 Jefferson Davis Highway, Suite 1204, Arlington, VA 22202-4302, and to the Office of Management and Budget, Paperwork Reduction Project (0704-0188), Washington, DC 20503.

1. AGENCY USE ONLY (Leave blank)	2. REPORT DATE December 2000	3. REPORT TYPE AND DATES COVERED Subcontract Report – May 5, 1999 to June 15, 2000

4. TITLE AND SUBTITLE
PVMaT Improvements in the BP Solarex Photovoltaic Module Manufacturing Technology, May 5, 1999 – June 15, 2000

5. FUNDING NUMBERS
C: ZAX-8-17647-05
Task: PVP1.6101

6. AUTHOR(S)
J. Wohlgemuth and S. Shea

7. PERFORMING ORGANIZATION NAME(S) AND ADDRESS(ES)
BP Solarex
Frederick, Maryland

8. PERFORMING ORGANIZATION REPORT NUMBER

9. SPONSORING/MONITORING AGENCY NAME(S) AND ADDRESS(ES)
National Renewable Energy Laboratory
1617 Cole Blvd.
Golden, CO 80401-3393

10. SPONSORING/MONITORING AGENCY REPORT NUMBER
NREL/SR-520-29459

11. SUPPLEMENTARY NOTES

NREL Technical Monitor: Richard L. Mitchell

12a. DISTRIBUTION/AVAILABILITY STATEMENT
National Technical Information Service
U.S. Department of Commerce
5285 Port Royal Road
Springfield, VA 22161

12b. DISTRIBUTION CODE

13. ABSTRACT *(Maximum 200 words)*

This is the annual report for a 3-year PV program to continue to advance BP Solarex photovoltaic manufacturing technologies to design and implement a process that produces polycrystalline silicon PV modules that can be sold profitably for $2.00 per peak watt or less, and which increases the production capacity of the Frederick plant to at least 25 megawatts per year. The accomplishments discussed in this report include: (1) developed processes to produce high-purity SiF_4 gas from a number of available commercial sources; (2) designed and implemented a new control system for casting; (3) verified relationship between higher minority-carrier lifetime in cast Si and cell efficiency; tracking material quality by measuring minority-carrier lifetime for each production casting; (4) reduced the wire-saw pitch to 450 microns with no loss in downstream yield; (5) demonstrated 8% improvement in average cell power on pre-production trial lots using PECVD silicon nitride; (6) developed a new EVA formation and demonstrated a 6-minute process to achieve adequate cure of PV modules in standard lamination equipment; (7) designed, purchased, and installed a new automated assembly line for large-area modules; and (8) implemented a factory-wide data collection and tracking system; production volumes and performance parameters are now monitored in real time through the local area network.

14. SUBJECT TERMS
PVMaT; modules; polycrystalline silicon; manufacturing; control system; minority-carrier lifetime; EVA

15. NUMBER OF PAGES

16. PRICE CODE

17. SECURITY CLASSIFICATION OF REPORT Unclassified	18. SECURITY CLASSIFICATION OF THIS PAGE Unclassified	19. SECURITY CLASSIFICATION OF ABSTRACT Unclassified	20. LIMITATION OF ABSTRACT UL